

Near-Eye Display and Tracking Technologies for Virtual and Augmented Reality

G. A. Koulouris¹, K. Akşit², M. Stengel², R. K. Mantiuk³, K. Mania⁴ and C. Richardt⁵

¹Durham University, United Kingdom

²NVIDIA Corporation, United States of America

³University of Cambridge, United Kingdom

⁴Technical University of Crete, Greece

⁵University of Bath, United Kingdom

Abstract

Virtual and augmented reality (VR/AR) are expected to revolutionise entertainment, healthcare, communication and the manufacturing industries among many others. Near-eye displays are an enabling vessel for VR/AR applications, which have to tackle many challenges related to ergonomics, comfort, visual quality and natural interaction. These challenges are related to the core elements of these near-eye display hardware and tracking technologies. In this state-of-the-art report, we investigate the background theory of perception and vision as well as the latest advancements in display engineering and tracking technologies. We begin our discussion by describing the basics of light and image formation. Later, we recount principles of visual perception by relating to the human visual system. We provide two structured overviews on state-of-the-art near-eye display and tracking technologies involved in such near-eye displays. We conclude by outlining unresolved research questions to inspire the next generation of researchers.

1. Introduction

Near-eye displays are an enabling head-mounted technology that immerses the user in a virtual world (VR) or augments the real world (AR) by overlaying digital information, or anything in between on the spectrum that is becoming known as ‘cross/extended reality’ (XR). Near-eye displays respond to head motion and allow for object manipulation and interaction. Having recently flooded the market, near-eye displays have the power to create novel experiences that potentially revolutionise healthcare, communication, entertainment and the manufacturing industries among others.

Two notable reviews of VR technologies in the 1990s by two pioneers in the field, Stephen R. Ellis and Frederick P. Brooks, outlined the fundamental challenges that existed back then, which, if solved, would enable the commercial success of XR technologies [Ell94, Bro99]. Although many of these challenges have been addressed, including low display cost, high resolution, low latency, 6-DoF tracking, complex rendering capability in real time and industry leaders entering the field, still, displays suffer from ergonomic, comfort, visual quality and interaction issues. Content for AR/VR is difficult and expensive to produce, and not yet abundant to the average non-technical consumer. As Ellis stipulated, because of unresolved display issues, VR had not yet found the ‘spreadsheet’ or ‘killer’ application, which would enable thousands of users to find solutions to previously intractable problems [Ell94]. What does

it take to go from VR ‘barely working’ as Brooks described VR’s technological status in 1999, to technologies being seamlessly integrated in the everyday lives of the consumer, going from prototype to production status?

The shortcomings of current near-eye displays stem from both imperfect tracking technologies as well as the limitations of the display hardware and rendering algorithms that cannot generate light that is perceived identically to naturally occurring light patterns. This is often the cause of conflicts in the human visual system. The major difference between traditional computer graphics and near-eye displays, is that whereas in computer graphics we often strive for photo-realism – aiming to *render like a camera would capture* – in near-eye displays, we aim for a physically correct *retinal* image, i.e., natural images or perceptual realism. On the bright side, the human visual system is also limited, allowing us to exploit these limitations to engineer displays that are perceptually effective, i.e., use visual perception as the optimising function for hardware and software design. Such an endeavour demands a multidisciplinary effort to develop novel near-eye display technologies, involving vision scientists, perceptual engineers, as well as software and hardware engineers.

In this state-of-the-art report, we analyse new advancements in display engineering that are driven by a broader understanding of vision science, which has led to computational displays for near-eye

displays. Today, such displays promise a more realistic and comfortable experience through techniques such as light-field displays, holographic displays, always-in-focus displays, multiplane displays and varifocal displays. New optical layouts for see-through computational near-eye displays are presented that are simple, compact, varifocal and provide a wide field of view with clear peripheral vision and large eyebox. Novel see-through rear-projection holographic screens and deformable mirror membranes enabled progress towards achieving more faithful visual cues. Fundamental trade-offs are established between the quantitative parameters of resolution, field of view and the form factor of the designs – opening an intriguing avenue for future work on accommodation-supporting near-eye displays.

We begin our discussion by reviewing principles of visual perception, acuity and sensitivity. We then describe the basics of light generation, image formation, wave and geometric optics, and then recall fundamental measures such as brightness, contrast, colour, angular/spatial/temporal resolution and dynamic range. We then contribute two structured overviews: First an examination of basic display types (transmissive, reflective, emissive) and near-eye display technologies (varifocal, multiplane, light-field displays, and holographic). We then review the tracking technologies involved for near-eye displays (mechanical, magnetic, inertial, acoustic, optical, hybrid) as well as tracking modalities such as head, eye, face/body, hands, multimodal and environment tracking. We conclude by outlining unsolved problems and challenges for future research.

2. Background

In this section, we provide the necessary background knowledge on human visual perception, light generation, optics and image formation relevant to the design of near-eye displays. We discuss tracking technologies and modalities as well as their applications relevant to near-eye displays in Section 4.

2.1. The Human Visual System

In this section, we describe the main principles of the human visual system (HVS). A visual stimulus in the environment passes multiple stages of the HVS before each of these stages determines how a stimulus is perceived by the user. Briefly, the HVS can be described as an iterative perceptual process (Figure 1) [Gol10b]. The process begins with a stimulus enters our eyes, constituting two visual fields, which enables us to process stereoscopic imagery over a field of view that encompasses zones with different stimuli sensitivities [WSR*17]. The optical system focuses the stimuli onto the *retina* (the ‘sensor’), which is connected to the visual pathways. This connection transports signals from the eye to the visual cortex in the brain, where the retinal signals are processed. The following steps, perception and recognition of the neural signals, allow us to finally understand what we see. Interestingly, perception (seeing something) and recognition (seeing a house) may happen at the same time or in reversed order [Gol10b]. Finally, the recognized stimulus results in an action, e.g. approaching the house. In the following, we briefly discuss physiological and perceptual properties of the HVS as well as relevant *limitations* of vision and perception.

More detailed information on exploiting the HVS for accelerated

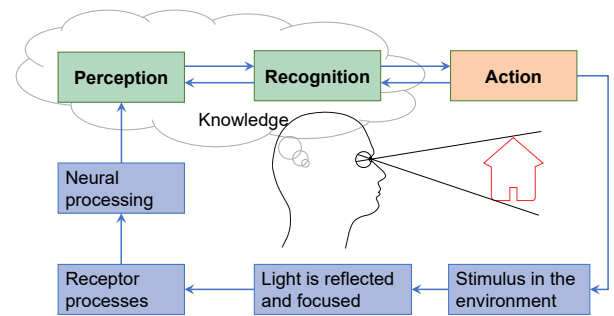


Figure 1: High-level model of the iterative perceptual process. After Goldstein [Gol10b].

rendering is given in the recent survey by Weier et al. [WSR*17]. Excellent information about human vision from a physiological point of view can be found in the book by Adler et al. [LNH*11].

2.1.1. HVS – Optical Properties

The HVS is characterised by several unique *optical* qualities that are a result of both the position and shape of the eyes. With binocular vision and both eyes looking straight ahead, humans have a horizontal field of view (FoV) of almost 190°. If eyeball rotation is included, the horizontal FoV extends to 290° [HR95, p. 32]. While the human eye will receive visual stimuli over the full extent of the FoV, the way stimuli are processed in different parts of the visual field is highly affected by the spatially varying properties of the retina. There are striking differences between central vision in comparison to the near and far periphery [CSKH90].

The distance between the pupils, the interpupillary distance (IPD), results in two streams of visual stimuli from slightly different perspectives, which are combined in the brain by a process called *stereopsis* and enables perception of depth also referred to as *stereo vision* [Pal99]. Depth perception is additionally enabled by visual cues such as parallax, occlusion, colour saturation and object size [CV95, HCOB10].

The spatial acuity of the HVS is limited by the eye’s optics. It is known from sampling theory that *aliasing* occurs if a signal contains frequencies higher than the observer’s Nyquist frequency [Sha49]. In human vision, this undersampling effect occurs for spatial frequencies higher than approximately 60 cycles per degree (cpd). Each cycle, also known as line-pair, denotes one black/white line pair taken together [Wan95, p. 24]. However, the eye’s optics in the cornea and lens act as a low-pass filter with a cutoff frequency around 60 cpd. This way, the signal that cannot be properly sampled and reconstructed is effectively removed through optical prefiltering.

The pupil is an additional important factor. With its adjustable diameter of 2 to 8 mm [Gol10a], it serves as an *aperture*. This adjustment mostly affects the sharpness of the image, as only about one magnitude of light intensity difference (1 log unit) can be controlled by the pupil. The eye’s adaptation to differences in brightness sensation (dark and light adaptation) mostly takes place on the retina.

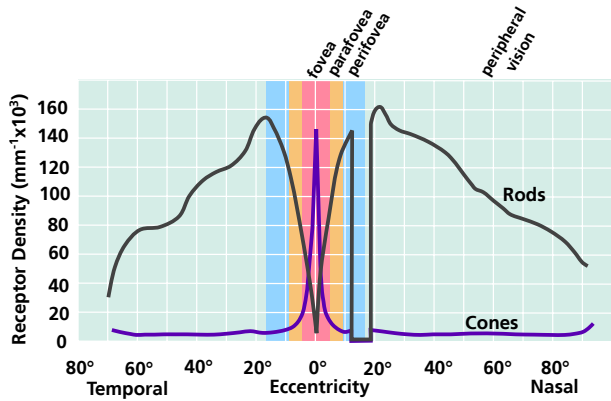


Figure 2: Retinal photoreceptor distribution. Image adapted from Goldstein [Gol10b, p. 51].

2.1.2. HVS – Receptor Processes

Light that enters through the eye is projected onto the retina, the photosensitive layer of the eye. This layer consists of two types of photoreceptors: $6 \cdot 10^6$ cones and approximately 20 times as many rods [Gol10b, p. 28]. Rods consist of only one type of light-sensitive pigment and are responsible for the brightness sensation in lower-light conditions (*scotopic* vision) by providing monochromatic feedback. Cones are divided into three types for different wavelengths, namely L-cones (long wavelengths), M-cones (medium wavelengths) and S-cones (short wavelengths). They are responsible for sensing colour and details in bright conditions (*photopic* vision). Photoreceptors of different types follow the distribution pattern shown in Figure 2. The central area of the retina, the *fovea* (approx. 5.2° around the central optical axis), consists entirely of cones. Cone density drops significantly with increasing eccentricities (the angular distance to the optical axis) [CSKH90] past the *parafovea* (approx. 5.2° to 9°) and *perifovea* (approx. 9° to 17°). These inner parts constitute *central vision*, while areas further away are referred to as *peripheral vision*. The highest density of rods is approximately $15\text{--}20^\circ$ around the *fovea*. Their density drops almost linearly. Just as the rods and cones have different densities across the retina, they have different spatial sampling distributions and follow a Poisson-disc distribution pattern [Yel83, Wan95, ch. 3]. The density of cones is related to *visual acuity*, the “keenness of sight”. The visual acuity of the eye drops significantly outside the small foveal region, where humans are able to generate a sharp image (acuity is already reduced by 75% at an eccentricity of 6°). Visual acuity can be expressed as minimum angle of resolution (MAR). Normal vision corresponds to 1 MAR, a measure describing that a feature size of 0.5 minutes of arc is still visible [LNH*11, p. 627]. This minimal feature size relates to a spatial frequency of a sinusoidal grating pattern of alternating black and white spaces at 60 cpd.

There are further factors influencing this keenness of sight. Visual acuity also depends on the contrast of the stimuli. The acuity limit is usually measured using a high-contrast image or a letter under photopic luminance conditions, which corresponds to typical daylight and display use cases. Moreover, the reduction of acuity depends on the overall lighting. Under dimmed light, the perceivable

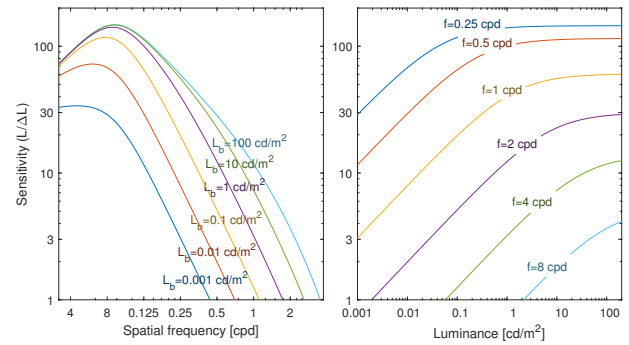


Figure 3: Contrast Sensitivity as a function of spatial frequency (left) and luminance (right). The plot is based on Barten’s model [Bar04].

spatial detail is reduced. The highest perceivable spatial frequency of a sinusoidal grating pattern reduces from ~ 60 cpd at photopic levels down to ~ 2 cpd for scotopic vision. In addition, contrast perception is affected [BSA91]. The eye’s sensitivity to contrast can be described by a contrast sensitivity function (CSF). The CSF describes the change in sensitivity as a function of stimulus size, background luminance, spatial frequency, orientation and temporal frequency. The CSF separately describes achromatic (luminance) and chromatic mechanisms ([L-M] and [S-(L+M)]). The CSF is defined as the reciprocal of the smallest visible contrast. The measurements are usually performed using sinusoidal grating patterns at different contrast levels. Figure 3 shows the variation in spatial frequency as a function of spatial frequency and luminance, respectively. The region under the curve is commonly called *the window of visibility* [LNH*11, pp. 613–621]. The resolvable acuity limit of (60 cpd) corresponds to the lowest contrast sensitivity value. Very high (>60 cpd) and very low frequencies (<0.1 cpd) cannot be perceived at all. While the upper limit can be explained by the cone spacing and optical filtering, the lower limit cannot be directly derived from the eye’s physiology [LNH*11, pp. 613–621]. Contrast sensitivity depends on the number of neural cells responding to the respective grating pattern [RVN78]. From the fovea to the periphery, sensitivity decreases significantly at all frequencies. The decrease is fastest for high frequencies [RVN78].

The varying distributions of rods and cones also affect the *sensitivity to colours* in different parts of the visual field [NKOE83]. The fovea is dominated by the cones sensitive to long and medium wavelength and capable of distinguishing between red and green colours. In contrast, only about 9% of our cones are responsible for the perception of short wavelengths, but they are more spread outside the fovea. This leads to a relatively higher sensitivity to blue colours in the periphery. Hence, contrast sensitivity also depends on the chromaticity of the stimulus. Blue/yellow and achromatic stimuli result in a less-pronounced decrease in terms of contrast threshold [Mul85]. The sensitivity to red–green colour variations decreases more steeply toward the periphery than the sensitivity to luminance or blue–yellow colours. Besides the different densities of the cones, neural processes are also of importance in this context [HPG09].

Retinal photoreceptors have the ability to adapt to stark changes

in light intensity. While adaptation to bright lighting can occur very rapidly, adapting to low lighting conditions takes considerably longer [Ade82, Bak49]. Adaptation influences the performance of the HVS, such as colour perception, spatio-temporal contrast sensitivity and the amount of perceivable detail [VMGM15, LSC04]. It enables humans to perceive visual information robustly over seven orders of magnitude of brightness intensities. However, we are not able to see equally well at all intensity levels: At lower light levels, due to rod-vision, acuity is reduced. During daytime, contrast sensitivity is lower, but visual acuity and colour vision excel. Similar to the drop of acuity with eccentricity that can be observed in stereopsis, depth perception is significantly reduced in the periphery [PR98].

2.1.3. HVS – Motor

Our eyes are constantly in motion. Six external muscles (the extraocular muscles) allow precise and fast changes of the horizontal and vertical orientation of the eye as well as torsional movements that bring the top of the eye toward the nose (intorsion) or away from the nose (extorsion). The primary goal of moving the eyes is to move the projection of the object of interest onto both foveae, so that the focused object is perceived with high detail. The most important types of motion are *saccades*, *fixations*, *vestibulo-ocular reflex*, *smooth pursuit eye motion*, and coupled *vergence–accommodation* motion. An excellent survey on the properties and effects of human eye motion from a psychophysical point of view is provided by Kowler [Kow11].

Saccades are the result of eye motion rapidly jumping from one region of interest to another. During a saccade, peak angular speeds of up to 900°/s [FR84] can be reached. Preceding the beginning of eye movement, there is a dramatic decline in visual sensitivity, which is referred to as *saccadic suppression* [VRWM78, WDW99, RMGB01]. As a result, during saccadic eye movements, accurate visual information cannot be acquired. In contrast, fixations describe the state and duration in which visual information is perceived while our gaze remains close to an object of interest. Fixation durations typically vary between 100 milliseconds and 1.5 seconds [WDW99]. It is assumed that the duration of a fixation corresponds to the relative importance and visual complexity of an area in the visual field. When viewing a typical natural scene, the HVS triggers around two to three saccades per second, and the average fixation time is about 250 milliseconds [KFSW09]. The spacing between fixations is, on average, around 7° of viewing angle. The unconsciously triggered tracking reflex when a moving object attracts our gaze is called smooth pursuit eye motion (SPEM). This motion enables the observer to track slow-moving targets so that the object is fixated onto the fovea. Interestingly, small eye movements up to 2.5°/s have hardly any effect on visual acuity [LNH*11]. However, the success rate depends on the speed of the target and decreases significantly for angular velocities in excess of 30°/s. Saccades are generally driven by position error, and smooth pursuit, generally, by velocity error. Both types of movements are generally binocular and involve both eyes rotating in the same direction. The eye is not a camera; the visual percept of a stable surround visual world is a perceptual construction of very small high-resolution snapshots and is due to a large degree to pervasive unconscious perceptual filling-in processes.

Stereopsis is highly entangled by *vergence* and *accommodation*.

In order to fixate an object, both eyes are required to simultaneously rotate in opposite directions (*vergence*). Accommodation is the mechanical ability of the eye to change the shape of the lens so one can focus at different distances [How12]. When the ciliary muscles at the front of the eye tighten, the curvature of the lens and, correspondingly, its focusing power is increased. Accommodation describes the natural counterpart of adjusting a camera lens so that an object in the scene is set into focus. Importantly, this process happens unconsciously and without any effort in less than a second at photopic illumination levels [Gol10a, p. 289]. Typically, stereoscopic displays drive *vergence* by providing binocular disparity cues using a separate image for each eye. Yet, as the images are shown on the screen, the eyes focus on the screen's distance. This can result in a conflict, known as the *vergence–accommodation conflict* [Gol10a, p. 1040]. Accommodation and *vergence* motions are coupled with the fixation process for binocular vision so that both eyes' gaze aims at the same point at which they focus.

2.1.4. HVS – Cortical processing

Retinal stimuli processing is followed by neural information processing in the *visual cortex* of the brain. Corresponding to the drop in the density of rods and cones, over 30% of the primary visual cortex are responsible for the central 5° of the visual field, while the periphery is under-represented [HH91]. Cognitive processing of images and perceptual differences between central and peripheral vision have been targeted by perception research. Thorpe et al. have shown that peripheral vision provides a rich source of information, crucial to the perception and recognition of contrast features, objects and animals [TGFTB01]. Furthermore, the HVS makes extensive use of contextual information from peripheral vision, facilitating object search in natural scenes [KKK*14]. Thereby, pre-processing of visual stimuli probably occurs. There is evidence that basic visual features (such as object size, colour and orientation) are pre-processed before actual attention is placed on the object by moving it into central vision [WB97]. Besides the process of stereopsis, the ability to interpret depth cues in the visual input to improve stereo vision and the sense of spatial localisation is highly entangled in the visual cortex.

Finally, vision is affected by cross-modal effects. In particular, VR systems often provide non-visual cues such as audio, vibration or even smell. These effects have been studied in psychological experiments on various interplays between cues [SS01, Pai05, SS03, WP04]. When sensory channels are substituted or combined, some implications occur: sensory channels are no longer seen as separate channels, but may affect each other through integration of sensory signals inside multimodal association areas in the brain [Pai05, LN07, Sut02, pp. 36–64].

2.1.5. HVS – Memory and Attention

The processing of visual information is highly dependent on knowledge and patterns stored in memory [KDCM15]. How such knowledge is stored is still a topic of fundamental research [SK07].

While attention is still not fully understood, research indicates that it has three components: (1) orienting to sensory events, (2) detecting signals for focused processing, and (3) maintaining a vigilant or alert state [PB71]. Attention is important for processing

visual stimuli and search behaviour [TG80]. It involves the selection of information for further processing and inhibiting other information from receiving further processing [SK07, p. 115]. Attention can occur in information-processing tasks in various ways [WC97]: *selective attention* is the choosing of which events or stimuli to process; *focused attention* is the effort in maintaining processing of these elements while avoiding distraction from other events or stimuli; *divided attention* is the ability to process more than one event or stimulus at a given point in time.

Being aware of the limitations of the human visual system enables us to avoid under- or over-engineering near-eye displays. In the following sections, we explore the theory that drives design choices in near-eye displays.

2.2. Light Generation

In this section, we examine the basic properties of light that contribute to image formation. Light can be modelled either as an electromagnetic wave or a stream of photons. In this state-of-the-art report, we focus on the wave nature of light that is more relevant to near-eye displays. When modelled as an electromagnetic wave, most forms of light generation relate to rapidly moving electrical charges consequently generating electromagnetic waves. Electromagnetic waves are self-propagating waves of intermittent electric and magnetic fields that carry energy, cyclically exchanged between the electric and magnetic components [YFF07]. The rate of exchange is the light frequency. A select range of frequencies, called the *spectrum*, can be perceived by the human eyes and is known as visible light. The wavelength λ of these frequencies relates to frequency via the equation $\lambda = c/f$, where c is the speed of light in vacuum and f is frequency. Visible light ranges from wavelengths of 380–780 nm or frequencies in the 10^{15} Hz range. Wavelength and amplitude of the light wave correspond to perceived colour and intensity, respectively [Pa199].

Forms of light generation include single charges, such as electrons, giving birth to photons. Electrons that change orbits in an atom release the *positive* energy difference as photons. This happens in semiconductors, such as light-emitting diodes (LEDs), where material properties define specific energy levels (bands) between which the electrons jump, generating light of specific wavelengths [MS08]. Another form of light emission is thermal emission, caused by the motion of atoms in solids, liquids and gases. Thermal emission usually contains photons spanning a wide range of energies, e.g., tungsten lamps [Pla13]. In the majority of VR/AR headsets, the modulated light is generated using LEDs and OLEDs (organic LEDs) [HB16].

LEDs are semiconductor chips selectively enriched with other material impurities (doped) to create a p–n junction, i.e., an interface between two types of semiconductors: one positive (p-side) and one negative (n-type) [MS08]. The p-side contains an excess of electron holes, while the n-side contains an excess of electrons enforcing the electrical current to pass through the junction only in one direction. Electron holes and electrons flow into the junction and when an electron meets a hole, the electron falls into a lower energy level, thus releasing energy in the form of a photon. LEDs are used both as a display backlight, in headsets that employ transmissive

liquid-crystal displays (LCDs), or directly integrated into silicon as individually addressable LED pixels in micro-LED displays [HB16]. Contrary to LEDs, OLEDs employ a thin film of organic compound that directly emits light in response to an electric current running through the electroluminescent layer [DF04]. Both micro-LED and OLED-based displays are expected to become affordable in the years to come.

2.3. Optics Principles

To make use of light in the context of a display, it has to be formed by optics. Depending on the phenomenon that we try to explain or exploit, we can formulate light travel and interactions as a wave in *wave optics* or simpler, as rays travelling in space using *geometric optics*.

Wave Optics Light as a wave is characterised by a particular wavelength, amplitude and phase [Goo17]. If two waves of the same frequency are *in phase* they are called *coherent*. Light consisting of one wavelength is called *monochromatic*. A consequence of that is that coherent light must also be monochromatic. Points of equal phase form a surface which is called a *wavefront*. The wavefront is spherical if waves are emitted from a point. If light is emitted from an infinite number of points on a plane, the wavefront consists of infinite planes that are orthogonal to the propagation direction, and is called a *planar wavefront*. Any complex wavefront can be formed from a collection of multiple virtual point sources and their spherical wavefronts. When a wavefront encounters an obstacle, the virtual point sources next to the obstacle's border transmit light behind the obstacle, a phenomenon known as diffraction [Luc06]. Diffraction depends on wavelength, as larger wavelengths diffract more [YFF07].

Geometric Optics When image points are far larger than the wavelength of light, geometric optics is typically considered. Geometric optics provide an abstraction that formulates light as travelling along straight lines (a.k.a. ray tracing), ignoring its wave nature. Geometric optics can describe simple optical elements, such as lenses, and geometric phenomena, such as reflection. Depending on material properties, light can be reflected, refracted, scattered, absorbed or diffracted by matter. For the purpose of this report, we will briefly discuss refraction and reflection. We refer the curious reader to more advanced books on the topic [YFF07, HB16].

Light changes direction when passing a border between two media of different optical densities due to the difference in speed of travel through these media, a phenomenon that is known as *refraction*. Let us consider a beam whose wavefront is perpendicular to the way of travel. When that beam of light meets the border of two different optical media, the edge of the wavefront that first enters the second medium and experiences a delay until the second edge also enters the medium, which causes a change in the wavefront angle, similarly to when a car moving from a pavement to mud at an angle, will rotate along its vertical axis. This happens because the first wheel will spin slower till the second wheel also reaches the mud. The amount of refraction depends on wavelength. The angle of deflection can be estimated using Snell's law for geometric optics [YFF07]. Short wavelengths travel slower in denser media, and

as such experience stronger diffraction – a phenomenon explaining why a glass prism disperses light into its spectral components. On the border of two materials, not all light is refracted. Some of it is always reflected and is polarised perpendicularly to the deflection angle. This partial light reflection at media boundaries can be calculated using the Fresnel equations [HB16].

The principles of most optical-image generation that is happening in near-eye displays heavily rely on geometric optics phenomena, such as refraction and reflection. For explaining holograms, though, a wave representation is needed. A detailed image formation model for the setting of holographic projection displays has been derived [PDSH17]. A model that includes diffractive light propagation and wavelength-dependent effects has also been proposed [SDP*18].

2.4. Image Formation

In this section, we explain fundamental display measures such as spatial, angular and temporal resolution, intensity, contrast and dynamic range. Most near-eye displays update information that is displayed in a raster-scanning fashion, reproducing pictures as a matrix of pixels arranged on a rectangular grid [HB16]. The image is formed by setting these pixels to different colours and intensities. The number and size of pixels in a given area of the screen determines the amount of information that can be displayed. The pixel size, and consequently pixel density, restricts the maximum size a display can have before its pixels can be individually discerned.

The viewing angle a single pixel occupies denotes the angular resolution of the display, which is of particular importance for near-eye displays. Human visual acuity can reach up to 60 cpd [Pal99], i.e., 120 pixels would be needed per degree of visual angle for them to be indiscernible. The temporal resolution of the display (refresh rate) denotes how many times per second a new image is drawn on the display. For near-eye displays, a refresh rate of ~90 Hz is desirable to eliminate flickering, especially in the periphery [TFCRS16].

Another essential display parameter is peak luminance, which is measured in cd/m^2 . The perceived brightness of a display depends on the energy emitted, the emission spectrum and the size of the image, among others. As the human visual system adapts to the overall intensity of a scene, display intensity levels should be at least as high as the display surroundings. If not, the image will appear faint and lacking contrast. In the real world, intensity levels span from 10^{-6}cd/m^2 up to 10^8cd/m^2 , a dynamic range of 14 orders of magnitude [MDMS05]. In headsets, display intensities usually span two to three orders of magnitude due to technical limitations, light reflections inside the headset or over the lens, etc. Dynamic range is especially problematic when liquid-crystal displays (LCDs) are employed, as the polarisers used in them always leak a small amount of light coming from the backlight [HB16]. High dynamic range (HDR) displays increase the span of displayable intensities, often by employing multiple spatial light modulators (SLM) stacked in series. For example, stacking an addressable LCD over an addressable LED display, usually of much lower resolution, allows for double modulation of light, increasing the bit depth of the output and achievable contrast [MMS15].

Most current headsets use 8-bit displays, which corresponds to

256 greyscale levels. Insufficient colour bit-depth often leads to visible brightness steps that are known as banding/contouring artefacts in areas that should otherwise appear smooth, an effect accentuated by the eyes' inherent contrast enhancement mechanisms [Rat65]. Displays' colour reproduction capabilities can be measured by defining their colour gamut [TFCRS16]. By marking the red, green and blue colour primaries used in a display on a chromaticity diagram and then joining those primary locations, the achievable colour gamut can be visualised [HB16]. Achieving wide colour gamuts requires narrow-band primaries (spectral) near the edges of the chromaticity diagram [TFCRS16].

2.5. 2D Spatial Light Modulators

The core component of any electronic display is a *spatial light modulator* (SLM), which controls the amount of light transmitted or emitted at different spatial positions and at a given instance of time. Here, we focus on SLMs that are commonly used in VR/AR displays: liquid-crystal displays (LCDs), liquid crystal on silicon displays (LCoS), and active-matrix organic light-emitting diode displays (AMOLED) [HB16].

While VR/AR tracking sensors often operate at 1000 Hz, the display refresh rates and response times are often much lower. For that reason, the most critical display characteristics in AR/VR are its temporal response and the quality of reproduced motion. The main types of artefacts arising from motion shown on a display can be divided into: (1) non-smooth motion, (2) false multiple edges (ghosting), (3) spatial blur of moving objects or regions, and (4) flickering. The visibility of such artefacts increases for reduced frame rate, increased luminance, higher speed of motion, increased contrast and lower spatial frequencies [DXCZ15]. To minimise motion artefacts, VR/AR displays often operate at higher frame rates and lower peak-luminance levels, and incorporate techniques that mask some of the motion artefacts.

LCDs rely on a transmissive SLM technology, in which a uniform backlight is selectively blocked to produce an image. The name of the technology comes from nematic liquid crystals, which form elongated molecules and can alter the polarisation of the light. The liquid-crystal molecules are trapped inside a sandwich of layers consisting of glass plates and polarisers. When an electric field is applied to the sides of the glass, the molecules change their alignment and alter the polarisation of the light, so that more or less light passing through the display is blocked by the polarisers. LCD is the dominant display technology at the moment, which has branched into numerous sub-types, such as twisted nematic (TN), multidomain vertical alignment (MVA), or in-plane switching (IPS). Those sub-types compete with each other in price, the quality of colour reproduction, viewing angles and dynamic range.

LCoS is another important technology based on liquid crystals, which can be found in projectors, but also some AR displays, such as the Microsoft HoloLens or the Magic Leap One. In contrast to LCDs, which modulate transmitted light, LCoS displays modulate reflected light. This is achieved by giving a reflective surface to a CMOS chip, which is then layered with liquid crystals, an electrode and a glass substrate. The light is typically polarised with a polarising beam-splitter prism, and colour is produced by sequentially

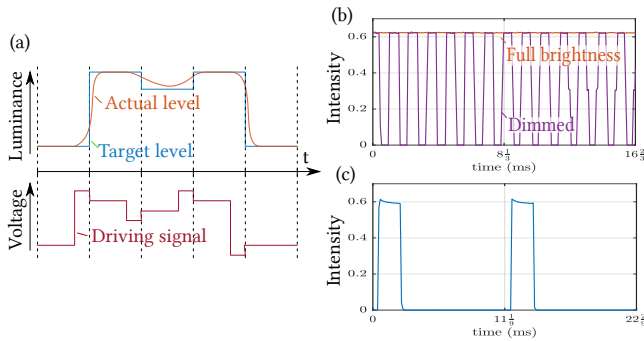


Figure 4: (a) Delayed response of an LCD, driven by a signal with overdrive. The plot is for illustrative purposes and does not represent measurements. (b) Measurement of an LCD (Dell Inspiron 17R 7720) at full brightness and when dimmed, showing all-white pixels in both cases. (c) Measurement of an HTC Vive display showing all-white pixels. Measurements taken with a 9 kHz irradiance sensor.

displaying images (fields) of different colours. Compared to LCD technology, LCoS SLMs are easier to manufacture, can achieve higher resolutions and can be made smaller. These are all desirable properties for any wearable near-eye display.

The liquid crystals found in the recent generation of LCDs and LCoS chips have relatively short response times and offer refresh rates of 120–240 Hz. However, liquid crystals still require time to switch from one state to another, and the desired target state is often not reached within the time allocated for a single frame. This problem is partially alleviated by over-driving (applying higher voltage), so that pixels achieve the desired state faster, as illustrated in Figure 4(a).

AMOLED displays are SLMs that emit light themselves when a voltage is applied. This brings many advantages, such as very high contrast (dynamic range), highly saturated (pure) colours, wide viewing angles, fewer components and thinner displays, as there is no need for a backlight or other light source. One of the remaining problems is the difficulty in driving AMOLED displays at high brightness when pixels are small (due to peak-current tolerance). They also tend to be more expensive to manufacture. However, the biggest advantage of AMOLED displays in VR/AR applications is their instantaneous response time. For that reason, AMOLED is the technology of choice for high-quality VR headsets, including HTC Vive and Oculus Rift, but also smartphones supporting Google Daydream headsets.

2.6. Motion Quality

While it may seem that fast response times should ensure good motion quality, response time accounts only for a small amount of the blur visible on LCD and AMOLED screens. Most of the blur is attributed to eye motion over an image that remains static for the duration of a frame [Fen06]. When the eye follows a moving object, the gaze smoothly moves over pixels that do not change over the duration of the frame. This introduces blur in the image that is integrated on the retina – an effect known as *hold-type blur*.

Hold-type blur can be reduced by shortening the time pixels are switched on, either by flashing the backlight [Fen06], or by inserting black frames (BFI). These techniques are known in the context of VR/AR displays as a low-persistence mode, in which pixels are switched on for only a small portion of a frame. Figure 4(c) shows the measurements of the temporal response for an HTC Vive headset, which indicates that the display remains black for 80% of a frame. The low-persistence mode also reduces the lag between the sensors and the display, as it shows only the first few milliseconds of a frame, for which the head-pose estimation is the most accurate. It should be noted that all techniques relying on rapidly switching the display on and off reduce the peak luminance of the display, and may also result in visible flicker.

See-Through Screens Researchers have explored see-through screen designs based on classical optical components. Hedili et al. [HFU13] describe a see-through microlens array for a headset display application. Soomro and Urey [SU16] report a see-through screen based on retro-reflectors for a head-mounted projection display application. Neither of these approaches has yet been redesigned for near-eye displays, nor for the expected diffraction effects accompanying that miniaturisation. Using silver nanoparticles and a front projector, Hsu et al. [HZQ*14] create a transparent screen that backscatters light at specific wavelengths. Yamamoto et al. [YYN*16] also describe a different approach to a wavelength-selective front-projection transparent screen using *cholesteric liquid-crystal dots*.

Curved and Freeform Screens Researchers have explored desktop-sized static, curved displays [WVSB10, HWC*17, BWB08, BKV11, KM15] and large-format, immersive, static curved displays [KLT*09, HKMA07, BW10, TNSMP17]. These displays are typically cylindrical or spherical in their surface profile. The work of Brockmeyer et al. [BPH13] demonstrated a static desktop-sized display. Researchers have also shown manually configurable flexible displays that use organic LEDs [YJK*10], thin electroluminescent films [OWS14], and electronic-ink [GHM*06]. Recently, a dynamically shape-changing display was demonstrated by Leithinger et al. [LFOH15]. For a more exhaustive survey on non-planar displays, we refer interested readers to the following papers: [ARS*18, LKKC17, RPPH12].

3. Immersive Near-Eye Display Technologies

Augmented reality and virtual reality using optical near-eye displays (NEDs) promise to be the next breakthrough mobile platform, providing a gateway to countless AR applications that will improve our day-to-day lives [BKLP04, vKP10]. Although most emerging consumer products are being advertised for gaming and entertainment applications, near-eye display technology provides benefits for society at large by providing a next-generation platform for education, collaborative work, teleconferencing, scientific visualisation, remote-controlled vehicles, training and simulation, basic vision research, phobia treatment, and surgical training [HS14]. For example, immersive VR has been demonstrated to be effective at treating post-traumatic stress disorder (PTSD) [DH02], and it is an integral component of modern, minimally invasive surgery systems, such as the da Vinci surgical system. Eye movement desensitization and

reprocessing has been shown by systematic clinical trials to also be effective for the treatment of PTSD, often combined with immersive VR [CLvdHE16]. We first review near-eye display optics in Section 3.1, in which we introduce the necessary optics terminology in Section 3.1.1, and also review optical designs both for VR and AR applications in Section 3.1.2 and Section 3.1.3, respectively. We dedicate Section 3.2 to accommodation-supporting near-eye display technologies. As an important emerging problem, we also provide a detailed overview of foveated displays in Section 3.3, and an overview of vision correction for near-eye displays in Section 3.4.

3.1. Near-Eye Display Optics

To fulfill the promise of immersive and natural-looking scenes, as described by Kress and Sterner [KS13b], designers of AR and VR NEDs need to solve difficult optical design challenges, including providing sufficient resolution levels, eyebox and field of view (FoV). A major impediment to achieving natural images, and a key cause of discomfort, is the vergence–accommodation conflict (VAC) [HGAB08, JPK*16, KBBDD17], which is caused by a mismatch between the binocular disparity of a stereoscopic image and the optical focus cues provided by the display (see discussion in Section 2.1.3). Mainstream strategies [Hua17] for tackling these challenges involve dynamic display mechanisms that can generate accurate visuals at all possible optical depths, which greatly increases the complexity of the NED design problem. Other obstacles to widespread adoption of AR NEDs include providing affordability, requiring a reasonable amount of computation and power, and providing a thin and lightweight form factor suitable for daily use. All of these problems are still waiting to be solved and even small steps towards a possible solution require a massive effort.

3.1.1. Near-Eye Display Optics Terminology

To provide a base for our review on optical NED technologies, we first summarise common optics terminology. The location of a depth plane (virtual image) generated by a near-eye display is typically reported in diopters, D , which corresponds to the reciprocal of the focus distance in meters ($D = \frac{1}{\text{meters}}$). Many standards exist for reporting binocular FoV, including starting from a specific point inside a person’s head or starting from a “cyclopean eye” between the user’s eyes (e.g., [WDK93]). Especially in the case of accommodation-supporting NEDs, the differing assumptions lead to widely varying estimates of the binocular FoV, and so we report only the well-understood measure of monocular FoV, which is typically reported in degrees. Resolution of a NED is quantified using cycles per degree (cpd). For a specific depth plane and visual field (portion of a FoV), typically cpd is reported in arcmins, which is $1/60$ degrees. The eyebox of a NED can be defined either as a volume or a plane, where the user’s eye can be located in front of a NED. Eyebox dimensions are typically reported in millimetres.

3.1.2. Near-Eye Display Optics for Virtual Reality

In the early 1800s, David Brewster introduced a hand-held stereoscope [Bre56] using a pair of photographs and a pair of magnifying glasses. Following Brewster’s optical layout, today’s most common commercially available near-eye displays employ a small screen and an optical relay to project light from the screen onto the user’s

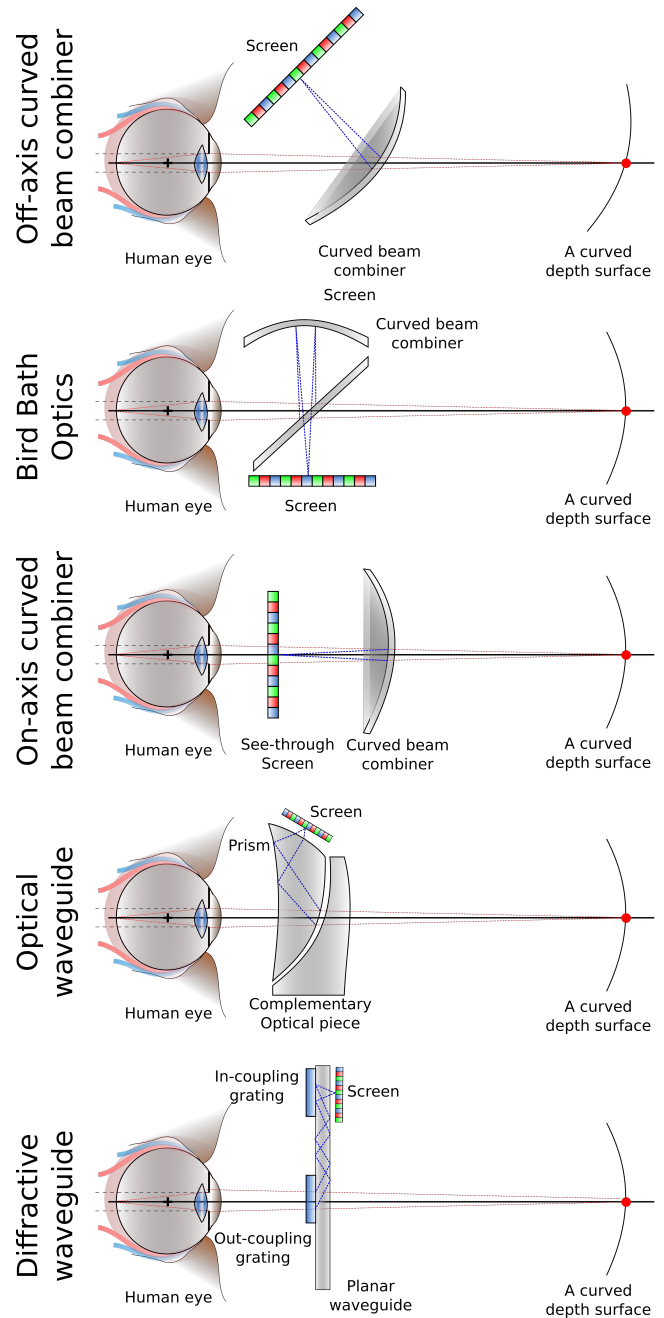


Figure 5: Diagrams showing various optical layouts for near-eye displays.

retinas, creating a magnified virtual version of the screen at a fixed depth. Some of these displays are made to be video see-through AR systems by displaying a view of the real world captured through an on-board camera [RF00]. In the next section, we review the optics of see-through near-eye displays that are illustrated in Figure 5.

3.1.3. See-Through Near-Eye Display Optics

Sutherland [Sut68] introduced see-through NEDs using a beam combiner near the eye of a subject to superimpose the direct view of the real world and computer-generated images. Optical systems relying on flat combiners have progressed greatly as described by Rotier [Rot89] and Cakmakci and Rolland [CR06]. The geometry of flat beam combiners along with the lenses used in optical NEDs dictates a strict trade-off: a large FoV quickly leads to a bulky form factor. Droessler and Rotier [DR90] propose a tilted catadioptric (reflecting and refracting) system to overcome FoV limitations by tilting the optics with respect to a flat combiner, and using a curved combiner as the final relay surface, which provides up to 60° of rotationally symmetrical monocular FoV. Tilted catadioptric systems are fundamentally limited in light efficiency, depend on a complex polarised optical system, and produce a bulky form factor. Gilboa proposes an off-axis single-element curved beam combiner [Gil91], and explores the associated optical design space. Today, modern variants of off-axis single-element curved beam combiners (e.g., Wang et al. [WLX16]) are deployed in military applications and consumer-level prototypes (e.g., Meta 2). Major limitations in off-axis single-element curved beam combiners come into play while extending FoV in horizontal directions when lit vertically; these combiners are known to provide poor imaging characteristics with eccentricity, and require a larger screen with a larger FoV demand.

Another family of see-through NEDs is based on waveguides. Cheng et al. [CWH09] propose a waveguide-based NED design that fuses curved beam combiners and waveguides into a single free-form prism. They describe a tiling strategy of these prisms to increase limited FoV, which requires multiple displays per prism. Flat combiners have been converted into thin cascaded waveguides as a see-through NED prototype (e.g., Lumus); however, FoV-related issues are still a major problem in practice. As described by Kress and Shin [KS13a], holographic methods simplify designing waveguides through holographic out-coupling and in-coupling of light. Today, such displays are present as consumer-level see-through NED prototypes (e.g., Microsoft HoloLens, Magic Leap One, Sony Smart Eye), which only report a maximum of 45° diagonal binocular FoV. Holographic optical elements (HOEs) can function as a complete reflective and diffusive beam combiner, as demonstrated by Li et al. [LLJ*16] and Maimone et al. [MGK17], with a small eyebox.

Retinal scanning displays propose to address each cell on a user's retina with a beam of light. Johnston et al. [JW95] first proposed a retinal-scanning NED by using laser light sources with a Micro-Electromechanical System (MEMS) scanner, which was later commercialized as well (Microvision Nomad). The eyebox generated by a retinal scanning NED is proportional to the size of the used mirror in the scanner, which therefore typically limit this aspect. Most recent developments in retinal NEDs were reviewed by Rolland et al. [RTB*16].

3.2. Accommodation-Supporting Near-Eye Displays

Accommodation-supporting NEDs [Hua17, Kra16] address the vergence–accommodation conflict (VAC) by matching the binocular disparity of virtual objects with correct optical focal cues for various depth planes. Figure 6 compares the optical layouts of

accommodation-supporting NEDs and Table 1 provides a comparison of their characteristics.

Varifocal Displays A simple solution for solving the VAC is a varifocal display, which dynamically changes the optical properties of the display. Although varifocal displays offer large computation benefits, they require precise gaze tracking. Liu et al. [LCH08] used a tunable lens system combined with a spherical mirror, demonstrating 28° of diagonal FoV with 10–14 cpd, which switches depth from 8 D to infinity (–0.1 D) within 74 ms. Another study by Konrad et al. [KCW16] also took advantage of an electrically tunable lens system, and demonstrated 36° diagonal FoV. Their solution allowed depth switching from 10 D to infinity (–0.1 D) within 15 ms, and provided 5–6 cpd resolution. Dunn et al. [DTT*17] provided a monocular FoV beyond 60° and a fast varifocal mechanism of 300 ms that switches depth from 5 D to infinity (–0.1 D). Most recently, Akşit et al. proposed using holographic optical elements as a part of an AR varifocal NED system [ALK*17a], offering a FoV of 60° with 18 cpd; however, the varifocal mechanism is still too slow at (410 ms) when switching from 5 D to infinity (–0.1 D). An evaluation of the effect of different HMD display configurations on discomfort can be found in Koulieris et al. [KBBD17].

Multiplane Displays Early on, Akeley et al. [AWGB04] demonstrated the benefits of a fixed-viewpoint volumetric desktop display using flat multiplanes, which allowed them to generate near-correct focus cues without tracking the eye position. Recently, such displays have been revisited with improved scene decomposition and gaze-contingent varifocal multiplane capabilities [NAB*15, MSM*17]. However, such displays have large power and computational demands, and require a complex hardware that would be difficult to miniaturise. These constraints limit their usefulness to perceptual experiments identifying the needs of future near-eye display designs. The work of Hu et al. [HH14] demonstrated a time-multiplexed multiplane display in the form of a wearable AR NED with a narrow field of view (30°×40°). Lee et al. [LCL*18] proposed a compact multiplane AR NED composed of a waveguide and a holographic lens, which demonstrated a FoV of 38°×19°. Zhang et al. [ZLW18] proposed a stack of switchable geometric phase lenses to create a multiplane additive light-field VR NED, providing approximate focus cues over an 80° FoV. Both the works of Lee et al. [LJY*18] and Hu et al. [HH14] demonstrated time-multiplexed multiplane AR NEDs with FoVs of 30° to 40°, respectively. Unlike all other previous work in multiplane approaches, most recently, Chang et al. [CKS18] demonstrated a fast-paced, (sub millisecond) multifocal display with an unprecedented 40 depth layers over a wide depth range (0.2–7 D) with 45° FoV.

Light-Field Displays Light-field NEDs promise nearly correct optical accommodative cues, but this comes at the cost of significant resolution loss. Lanman and Luebke [LL13] introduced a VR near-eye light-field display (NELD) that uses microlenses as the relay optics, showing a prototype with a FoV of 29.2°×16.0°, leading to a resolution of 2–3 cpd. Huang et al. [HCW15] developed VR NELDs further, demonstrating a prototype with a diagonal binocular FoV of 110°, leading to a resolution of 3–4 cpd. Akşit et al. [AKL15] created a VR NELD using a pinhole mask in front of an AMOLED display, and demonstrated full-colour images with a diagonal binocular

Display technique	Focus mechanism	See-through	FoV	Resolution	Eyebox	Form factor	Compute overhead	Gaze tracking
Pinlight displays [MLR*14]	light fields	yes	wide	low	small	thin	high	no
Freeform optics [HJ14]	light fields	yes	narrow	high	moderate	moderate	high	no
HOE [JBM*17]	light fields	yes	moderate	low	large	moderate	high	yes
HOE [MGK17]	holographic	yes	wide	moderate	small	N/A	high	yes
Focus tunable light engine [LCH08]	varifocal	yes	narrow	moderate	small	bulky	moderate	yes
Multifocal plane display [HH14]	multifocal	yes	narrow	moderate	moderate	bulky	high	yes
Membrane [DTT*17]	varifocal	yes	wide	low	large	bulky	low	yes
Varifocal HOE [ALK*17b]	varifocal	yes	wide	moderate	large	moderate	low	yes
Multifocal display [LCL*18]	multifocal	yes	narrow	low	large	thin	high	no
Focal-surface display [MFL17]	focal Surface	no	narrow	moderate	narrow	moderate	high	no
Application-adaptive foveated display [ACR*19]	focal surface	yes	wide	moderate	large	moderate	low	no

Table 1: A comparison of see-through accommodation-supporting near-eye displays, including the virtual reality near-eye display implementation of Matsuda et al. [MFL17]. This table is modelled after those in Dunn et al. [DTT*17], Akşit et al. [ALK*17b] and Matsuda et al. [MFL17]. Note that, in our chart, a moderate FoV is defined as 40–60°, moderate resolution is defined as 10–20 cpd, and a moderate eyebox is defined as 5–10 mm. Moderate values are adapted from [CR06, MFL17].

FoV of 83° with 2–3 cpd. By using a see-through sparse backlight mechanism, Maimone et al. [MLR*14] introduced a single-colour prototype with a diagonal FoV of 110° and a resolution of 2–3 cpd.

Static and Dynamic Holographic NEDs Holography promises an accurate representation of four-dimensional (4D) light fields; however, the limitations of such displays include a small eyebox, large computational demand, long calibration times, and the design trade-off between limited resolution or a bulky form factor. Static holograms encoded into HOEs have been used in various NED types as optical combiners [JBM*17, MGK17, LCL*18] or projection surfaces [ALK*17a], although the static holograms in these displays do not provide 4D light fields. On the other hand, dynamic holographic VR NEDs can be achieved using phase-only spatial light modulators, which can encode holograms [SHL*17, MGK17, MFL17], enabling a glasses-like form factor and a wide FoV (~80°).

3.3. Foveated Displays

To match 20/20 acuity across the full field of view, a near-eye display would need to provide 400 megapixel resolution [SM16]. However, driving a display at this resolution requires too much bandwidth, power and computation to be feasible. The retinal cone distribution of the human eye leads to high spatial sensitivity only in the fovea (see Section 2.1.2). By combining a low-resolution image in the user's periphery with a high-resolution inset in the fovea, a *foveated display* can better match the display's output to the human visual system's performance, thus reducing bandwidth, power and computation requirements substantially.

Foveated NEDs promise a major increase in simplicity while relying on gaze trackers. We start by reviewing optical hardware in the foveated display literature. The earliest example of a gaze-contingent visual stimulus was presented by Reder in 1973 [Red73], paving the way for further research into foveated imagery. Later on, the first proposal for foveated display hardware appeared in the work of Baldwin et al. [Bal81] as a variable resolution transparency magnified by large concave mirrors. A year later, Spooner et al. [Spo82] showed another style of desktop foveated hardware, which combines two different displays to provide high-resolution images at the fovea, and low-resolution images in the periphery. To our knowledge, the work of Shenker et al. [She87] is the first to realise the concept of

combining two different displays in a near-eye display configuration, in the form of a steerable foveal inset with 20 cpd resolution created using fiber-optics and pancake-type optical relays. Later, the work of Howlett et al. [How92] followed the path of combining two different displays in an NED configuration to build a complete telepresence system with cameras. Rolland et al. [RYDR98] combined two displays using a beam splitter in a NED setting. In their design, a high-resolution inset with 24 cpd resolution is relayed to the fovea of the eye using microlenses with a FoV of 13.30°×10.05°, while a lower-resolution display at 6 cpd spans across a FoV of 50°×39° through a magnifier lens. Godin et al. [GMB06] describe a dual projector layout in order to realise a stereoscopic desktop-sized display with a fixed foveal region. Mauderer et al. used gaze-contingent depth of field blur (gcDOF) to reproduce dynamic depth of field on regular displays, providing an alternative way of conveying depth [MCNV14]. Recently, Lee et al. [LCL*18] proposed a compact AR NED comprised of a waveguide and a holographic lens that combines two displays. Their design has a FoV of 38°×19° and eliminates the needs for gaze-tracking hardware. Most recently, Akşit et al. [ACR*19] demonstrated that printed optical components can be used to create static focal surfaces with fixed and dynamic foveation support for near-eye displays with 12 cpd, spanning across a FoV of 55°×30°. There is undoubtedly a clear hardware benefit in foveation; we refer curious readers to the following set of papers for the discussion of detailed perceptual and computational benefits of foveation in computer graphics: [PN02, PSK*16, KSH*17].

3.4. Vision-Correcting Near-Eye Displays

For users who need corrective lenses in their everyday lives (i.e., 'near-sighted' or 'far-sighted'), the situation is even more complex, because these users already have to deal with the vergence–accommodation conflict (VAC) even without AR or VR [SHL*17]. Consider a 'near-sighted' user who can comfortably verge and accommodate to, say, 0.5 m, but needs corrective lenses to focus clearly on objects at 10 m. When they first use the corrective 'distance' lenses, an object at 10 m appears in focus (because to their eyes, it is at 0.5 m, but they will verge to 0.5 m, giving 'double vision'). Only after many hours, days or even weeks of wear, does the vision system gradually adapt to verging at 10 m, while still accommodating to 0.5 m. Some users never become adapted to such a large VAC [AKGD17]. Over generations, opticians have empirically stud-

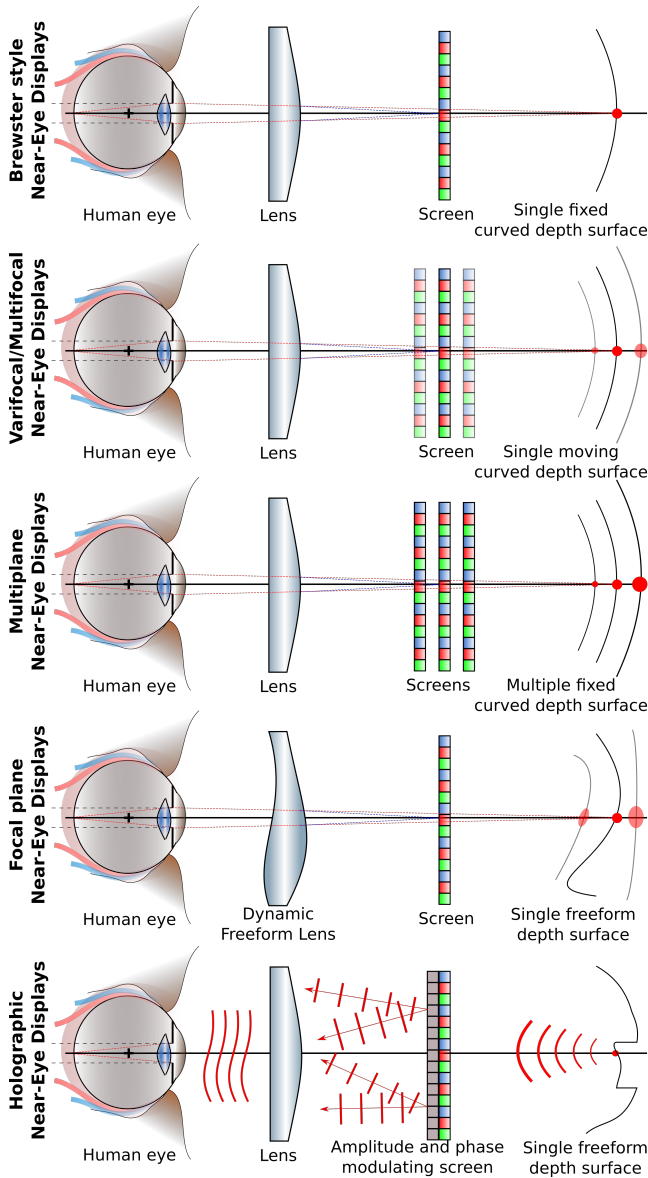


Figure 6: Diagrams comparing generic optical layouts for various different types of accommodation-supporting near-eye displays with a traditional Brewster-style near-eye display layout [Bre56]. Accommodation-supporting near-eye displays can be classified as varifocal/multifocal, multiplane, focal surface, and holographic near-eye displays.

ied the range of VACs (‘zone of clear single binocular vision’, ‘zones of comfort’ [DM64, Fry39]), which are tolerable and to which most users can adapt.

When donning a near-eye display, users requiring vision correction still need to wear their corrective lenses. A few AR displays, such as the Lumus DK-32, provide a physical space between the user’s eyes and the display for fitting prescription lenses. For presbyopes (people over about 40 years of age), who account for about 40%

of US population, this does not solve the problem because the user’s range of focus is restricted by the focus range of the lenses being worn at any moment – for instance “reading” glasses or “driving” glasses. Installing bifocals, trifocals, or progressive lenses merely puts a particular distance in focus at one vertical angle, forcing the user to tilt their head up or down to bring into focus a real-world object that is at a particular distance. Even the most recent offerings require the user to turn a focus knob on the lens (e.g., Alvarez lens) to adjust the depth of the focal plane – an unacceptably awkward requirement for most users.

We envision a future in which high-quality mixed-reality experiences can be realised for all users, regardless of prescription, in an efficient, cost-effective way. This requires to accessibility technologies, such as corrective lenses, to be more tightly integrated into the display.

Recently, a very promising body of work has become available on prescription correction in near-eye displays [CDAF18, PKW18, LHG*18]. These methods allow for automating per-user image modifications using all or some of the following hardware: (1) a pair of focus-changing optical layouts for partially or globally changing the optical power of the real world [MN15], (2) a gaze-tracking mechanism to predict where a user is looking at, and (3), a depth sensor or a pair of conventional cameras to interpret real-world depths in front of the user, increasing the accuracy of gaze estimations.

Another camp on tackling vision correction is through convolutional methods [MGDA*15, HWBR14]. This approach has been heavily researched in the most recent years [IK15, IAIK16], and found to be requiring a large calibration effort with respect to focus-changing optical layouts.

Another vision correction methodology that is important for near-eye displays is along the axis of colour correction, which colourblind people can take advantage of. A body of work has investigated colour correction in augmented reality using transparent spatial light modulators [LSZ*18, WHL10] and projectors [ABG10]. Such additions to near-eye displays require a rethinking of optical design; therefore, a combination of all previous efforts are still yet to be researched.

4. Tracking Methods for Near-Eye Display Technologies

Sherman and Craig [SC18] define the four key elements of virtual reality (which for them encompasses augmented and mixed reality) to be:

1. **Virtual world** comprises the virtual content of a given medium.
2. **Immersion** is the replacement of perception with virtual stimuli.
3. **Sensory feedback** based on the user’s physical position in space.
4. **Interactivity** is responding to the user’s actions.

Providing correct sensory feedback therefore requires measuring, or *tracking*, the location and orientation of the head-mounted display relative to a known reference frame, so that the VR system can respond by rendering the correct images to be displayed to the user. Figure 7 illustrates this standard input–output cycle of VR and AR systems. To provide meaningful interactivity, it is not only necessary to track the head-mounted display, but it is also necessary to track

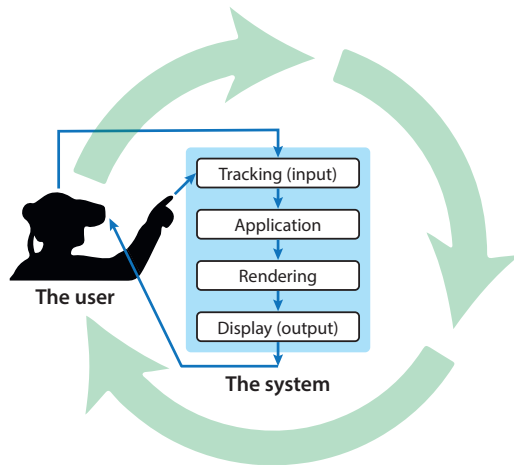


Figure 7: The VR/AR system input–output cycle according to Jerald [Jer09]. The user’s motion is tracked, the application reacts to the motion and renders visual content for immediate display.

the user, their motion and their environment, so that their actions can trigger appropriate responses.

In this section, we are therefore considering the full range of tracking techniques, from head tracking for determining the headset’s pose, to tracking of the user’s body pose, their hands, facial expressions and eye gaze, as well as the environment. We first briefly look at the underlying tracking technologies in Section 4.1 and discuss their pros and cons, including their accuracy and latency, as well as their suitability for different tasks. See recent surveys [BCL15, MUS16] for a more detailed account. We further discuss recent progress across different tracking modalities in Section 4.2, and how this informs the design of state-of-the-art VR and AR systems in Section 4.3.

4.1. Tracking Technologies

Convincing and immersive virtual or augmented reality requires the real-time tracking of the user’s head-mounted display as well as their interaction with the world [BCL15]. Over the last few decades, many tracking approaches have been proposed, based on different tracking technologies as well as combinations of multiple technologies (see examples in Figure 8). Each approach needs to find a trade-off between key performance criteria [WF02], such as accuracy, update rate, latency, jitter, noise and drift, and other considerations such as visibility requirements, contact-based versus contact-free, and active versus passive methods.

One important property of tracking approaches is how many degrees of freedom, or DoF, they can measure. The position and orientation of an object can be uniquely specified using six degrees of freedom (see figure to the right): 3 DoF for translation (left–right,

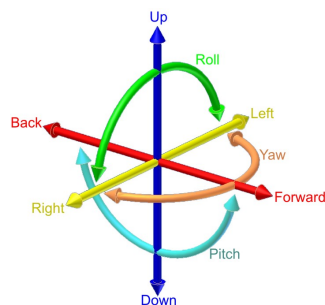


Figure 9: 6 degrees of freedom.

up–down, forward–backward) and 3 DoF for rotation (pitch,

yaw, roll), for a total of 6 DoF.

Some approaches only recover

the three rotational DoF, so that a viewer can look around a virtual world from a fixed viewpoint. Only 6-DoF tracking allows the viewer to move in the virtual world like in the real world.

Mechanical Tracking is one of the oldest approaches that has been used at least since Ivan Sutherland’s ground-breaking head-mounted display [Sut68]. Using a mechanical arm with sensors at the joints, position and orientation can be measured with high accuracy and low jitter and latency. The main limitation is that the mechanical arm needs to be physically connecting the object of interest to a fixed reference frame, such as connecting Sutherland’s display to the ceiling, or a joystick to a desk. This limits the range of possible motions to the fixed location at which the system is installed. However, this may be acceptable or even desirable in certain application scenarios such as location-based entertainment.

Magnetic Tracking measures the magnetic field vector using three mutually orthogonal magnetometers or electromagnetic coils [RBSJ79]. Magnetometers measure static magnetic fields, such as the Earth’s natural magnetic field, which provides a 3-DoF orientation measurement. Electromagnetic coils can be used to measure the current induced by an active source, and three sources are sufficient for full 6-DoF pose estimation. Another main benefit of magnetic tracking is that no line of sight is required, which is why it is for example used by the Magic Leap One AR headset and controller [BLW*17]. However, magnetic tracking tends to be sensitive to metal as well as fairly noisy and expensive. Recently, centimetre-level accuracy has been demonstrated using only commodity WiFi infrastructure [KK17, ZLAA*18].

Inertial Tracking relies on accelerometers and gyroscopes to estimate velocity and orientation. This functionality is often grouped into inertial measurement units (IMUs), which have become popular since the introduction of microelectronic mechanical systems (MEMS) that offer a cheap and small package with a high update rate. The biggest weakness of inertial tracking is drift, as measurements need to be integrated once to obtain orientation and twice to obtain position, which leads to significant drift over time. In practice, MEMS IMUs often also include magnetometers to reduce rotational drift, e.g., as used in the Oculus Rift development kit [LYKA14] or Google’s Daydream headset, which both only support 3-DoF orientation tracking. Many practical implementations combine IMUs with other tracking techniques (see ‘hybrid tracking’) to manage drift while benefitting from the high update rate.

Acoustic Tracking measures distances using time-of-flight or phase-coherent ultrasound waves [Sut68]. Devices are generally small and cheap, but suffer from low accuracy and refresh rates, and require line-of-sight while only providing 3-DoF orientation. For these reasons, acoustic tracking is becoming less common, although it is still being used for room-scale environments [SAP*16].

Optical Tracking uses one or more cameras in the visual or infrared spectrum to reconstruct the position and/or orientation of

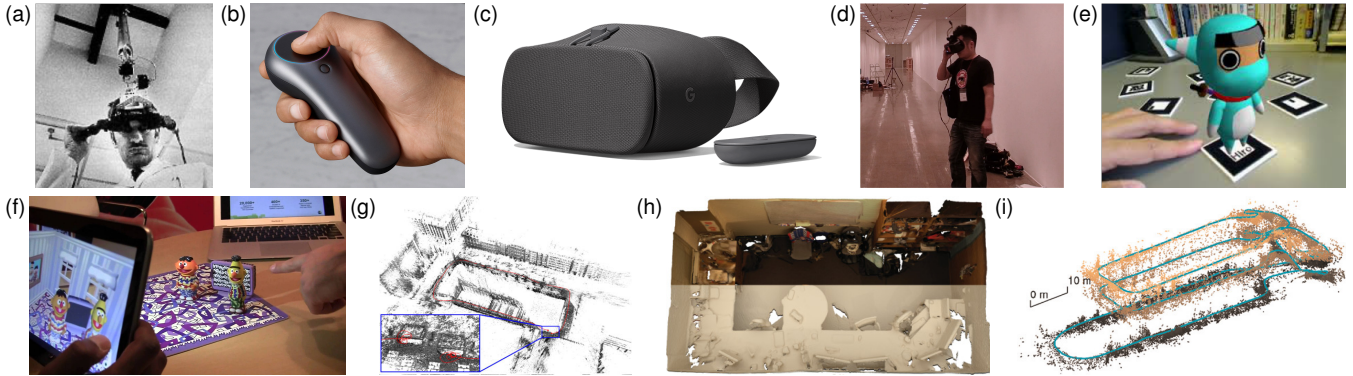


Figure 8: Example uses of the tracking technologies discussed in Section 4.1: (a) Sutherland’s ‘Sword of Damocles’ mechanical tracker (1968) [Sut68]; (b) the Magic Leap One Controller (2018) uses magnetic tracking [BLW*17]; (c) Google Daydream View (2017) uses inertial tracking for 3-DoF localisation of headset and controller; (d) ultrasonic tracking for room-scale 6-DoF localisation [SAP*16]; (e) marker-based optical tracking using ARToolkit [KB99]; (f) model-based optical tracking using Vuforia; (g) SLAM-based tracking using direct sparse odometry [EKC18]; (h) depth-based tracking using BundleFusion [DNZ*17]; and (i) visual-inertial odometry [LLB*15] as a hybrid technique combining optical and inertial tracking.

objects relative to the camera or, alternatively, the camera’s pose relative to the environment as used in AR [BCL15, MUS16]. A huge range of different optical tracking approaches and technologies have been proposed in recent years. They all rely on image processing and computer vision to interpret the captured images or videos. (1) *Marker-based* tracking approaches look for known artificial markers, such as retro-reflective spheres used for traditional motion capture (e.g., Vicon), or 2D fiducial markers like ARToolkit [KB99] that enable 6-DoF camera pose estimation. (2) If the geometry of the scene, or objects in it, is known, it can also be used for *model-based* tracking. A special case of this is the tracking of a planar surface, as it simplifies the pose estimation based on estimated homographies [MUS16]. (3) *SLAM-based* tracking performs simultaneous localisation and mapping in previously unknown environments. SLAM techniques have been covered thoroughly in two recent surveys [CCC*16, SMT18]. (4) *Depth-based* tracking uses depth maps acquired from infrared-based depth sensors that have become widespread over the last decade. Such sensors usually operate using the active stereo [Zha12] or time-of-flight [KBKL10] principle (e.g., Microsoft Kinect and Kinect One, respectively). Overall, most optical tracking approaches are usually very accurate, reasonably cheap, immune to metal and work over long ranges. However, they do require a line of sight, some techniques require specific markers, and update rates can be low (10s of Hz).

Hybrid Tracking combines multiple tracking technologies to overcome the limitations of each one, as no single tracking technology provides a silver bullet [WF02]. A common combination is visual-inertial SLAM [LLB*15], which fuses SLAM-based tracking (high accuracy, but low update rate) with inertial tracking (high update rate, but long-term drift) to reduce latency and increase accuracy and robustness. This is for instance used by the Microsoft HoloLens and Windows Mixed Reality HMDs [ESS*16], as well as Apple’s ARKit and Google’s ARCore AR APIs. Valve’s Lighthouse system is another hybrid tracking technology that combines optical tracking (using a swept infrared laser) for high-accuracy positioning with in-

ertial tracking for low-latency tracking [YS16]. Hybrid systems have shown the best overall tracking performance, but are necessarily more complex and expensive than any single technology.

4.2. Tracking Modalities

Tracking the user and their interaction with the real and virtual worlds comes in many flavours. Now that we have looked at the arsenal of tracking technologies that are at our disposal, we will next explore some recent advances in specific tracking modalities (see examples in Figure 10). We start with head and eye tracking, which both provide invaluable information about what imagery to show to the user. Next, we expand the tracking of the user by tracking their full body, hands and face. Finally, we are taking a quick look at current techniques for reconstructing static and dynamic environments, with which the user may be interacting while wearing a near-eye display.

Head Tracking In the beginning, there was only head tracking [Sut68], although Sutherland proposed both a mechanical and an ultrasound-based head tracker. This early work clearly demonstrated how important knowing the head pose is for rendering images that appear fixed in 3D space. Great advances in tracking technology over the last 50 years have led to widely available commercial near-eye displays that have head tracking built in, such as the Oculus Rift, which relies on IMUs [LYKA14] in combination with infrared-based optical tracking. Recent research prototypes have also successfully experimented with using a cluster of rolling-shutter cameras for kilohertz 6-DoF visual tracking [BDF16], using a single RGB-D camera [TTN18] or most simply a standard RGB camera [RCR18].

Eye Tracking aims to estimate the gaze direction of a user – ideally for both eyes, so that the 3D point at which both eyes are verging can be determined [WPDH14]. Eye trackers can be desk-mounted [WPDH14], laptop-mounted [ZSFB19], head-mounted [SB15] or using the front-facing camera of mobile phones and

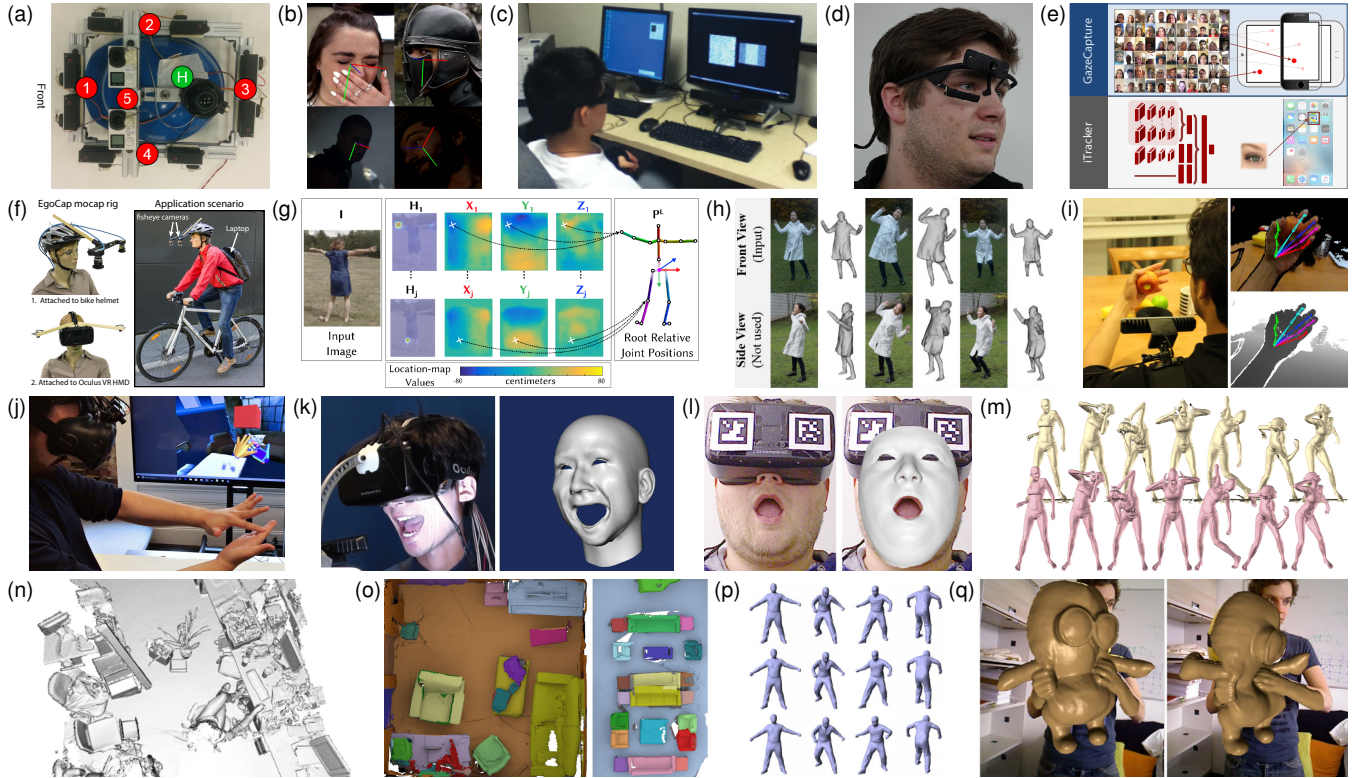


Figure 10: Examples of the tracking modalities discussed in Section 4.2: (a) head tracking with five pairs of rolling shutter cameras at kilohertz frequencies [BDF16]; (b) image-based head tracking [RCR18]; (c) desk-mounted eye tracker below the display [WPDH14]; (d) head-mounted eye tracking [SB15]; (e) phone-based eye tracking using deep learning [KKK*16]; (f) egocentric inside-out motion capture [RRC*16]; (g) live motion capture from a single video camera [MSS*17]; (h) performance capture from monocular video [XCZ*18]; (i) egocentric hand tracking from an RGBD camera [MMS*17]; (j) tracking multiple interacting hands for VR [TTT*17]; (k) head-mounted face tracking using measure sensors [LTO*15]; (l) face tracking from a RGBD camera [TZS*18]; (m) performance capture of full bodies and hands [RTB17]; (n) static environment reconstruction by KinectFusion [NDI*11]; (o) annotated 3D scene reconstruction [DCS*17]; (p) non-rigid motion tracking and surface reconstruction [GXW*18]; and (q) real-time volumetric non-rigid reconstruction [IZN*16].

tablets [KKK*16, KAB18]. Near-eye input avoids the problems of head pose and eye-region estimation, and allows use of high-resolution images of the eye. Most eye trackers work in the infrared spectrum as dark irises appear brighter in it and the corneal reflection can be filtered out by an infrared bandpass filter, resulting in stronger contrast to the black pupil that is used for gaze estimation.

In the following, we briefly summarise the history and state-of-the-art approaches for video-based eye tracking. We ignore other invasive eye tracking technologies such as scleral coil trackers. Duchowski’s book on eye tracking methodology [Duc17] provides more practical information for the interested reader. In addition, curious readers can read a detailed up-to-date survey of gaze-tracking systems and gaze-estimation algorithms in the work of Holmqvist et al. [HNA*11] and Kar and Corcoran [KC17].

Feature-based gaze-estimation methods locate the pupil and then map the pupil location to a screen location using user-specific calibration. The most recent pupil detection algorithms are discussed in this section. The Starburst algorithm [LWP05] iteratively locates the pupil center as the mean of points which exceed a differential lu-

minance threshold along the rays extending from the last best guess. In the SET method [JHB*15], the convex hull segments of thresholded regions are fit to sinusoidal components. Świrski et al. [SD14] and Pupil Labs [KPB14] both start with coarse positioning using Haar features. Świrski et al. then refine by k-means clustering the intensity histogram and a modified RANSAC ellipse fit, while Pupil Labs use ellipse fitting on connected edges. ExCuSe [FKS*15], ElSe [FSKK16], and PuRe [SFK18] use morphological edge filtering followed by ellipse fitting. PuRe is capable of selecting multiple edges for the final fitting and edge selection. ExCuSe and ElSe provide alternative approaches for cases when edge detection is not applicable. Recently, Fuhl et al. [FGS*18] presented circular binary features (CBF) to learn conditional distributions of pupil positions for the datasets on which they test. These distributions are indexed by binary feature vectors and looked up at inference time.

Due to the success of deep learning methods in many areas of computer vision, the state-of-the-art algorithms are mostly based on convolutional neural networks (CNNs) [SMS14, WBZ*15, GWW*16, HKN*16, KKK*16, WBM*16, MBW*17, PZBH18,

PSH18, KSM*19]. Networks with more layers generally outperform shallower ones, and VGG16 [SZ15] is emerging as a consensus architecture to be wrapped with preprocessing or context-aware layers [ZSFB19]. Kim et al. propose a network architecture for low-latency and robust gaze estimation and pupil localization [KSM*19]. PupilScreen measures the pupil diameter with a CNN from single smartphone photo of the eye [MBW*17]. Additionally, other approaches differing from the aforementioned ones are appearance-based methods, which directly compute the gaze location from the eye image [WBZ*15, ZSFB15, TSSB17].

Related work on remote gaze tracking includes training across multiple cameras [ZHSB18], using the screen as a glint source [HLNL17], using corneal imaging for fixation extraction and activity detection [LK18], and machine learning for calibrating trackers [SFK17]. Tonsen et al. [TSSB17] explore gaze tracking using combinations of multiple low-resolution and low-power miniature cameras, which is a favourable condition for mobile hardware.

Full-Body Tracking estimates human body pose in terms of a kinematic skeleton, which comprises rigid *bones* that are connected at *joints* with varying degrees of freedom [MHKS11]. Most commercial motion-capture systems use optical tracking with multiple cameras, either using markers (e.g., Vicon, OptiTrack) or markerless (e.g., The Capture, iPi Soft), while some systems use IMUs (e.g., Xsens, Neuron), which are not constrained to a fixed capture volume. Motion capture has also been demonstrated using a single consumer depth camera, such as the Microsoft Kinect [WZC12, SGF*13], which has the benefit of being largely invariant to the colour of clothing being worn. Approaches that use body-mounted cameras overcome the restricted capture volumes of previous approaches [SPS*11] and also enable motion capture in space-constrained environments [RRC*16] that were previously infeasible for optical tracking approaches. Most recently, deep learning applied to large datasets has enabled monocular motion capture from a single camera [ZZP*18], even live and in real time [MSS*17, XCZ*19]. In contrast to motion capture, performance capture aims to reconstruct the surface geometry of humans, not just their skeletons [TdAS*10]; this surface reconstruction is more desirable for virtual reality applications, as this would enable one to see their own body in the virtual world. Recent monocular approaches have shown convincing results with a depth sensor [DDF*17] or just a standard video camera [XCZ*18].

Hand Tracking aims to reconstruct the pose of hands and fingers, which are crucial for our everyday interaction with the real world. Hand tracking is a challenging problem because fingers look very similar and tend to occlude each other. Most hand-tracking approaches use optical tracking, as it works from a distance with line-of-sight. The wrist-worn Digits sensor uses a custom infrared projector-camera system [KHI*12], but most approaches use commodity hardware instead, particularly consumer depth cameras. The colour channel is sometimes used for hand segmentation [OKA11], but many approaches only use the depth channel [SMOT15, TBC*16, TPT16], as it is invariant to skin colour and illumination, which makes colour-only hand tracking more challenging [MBS*18]. Egocentric approaches use body-mounted RGB-D cameras instead [RKS*14, MMS*17] to recover hand pose

from the user's viewpoint. While most work focuses on tracking a single hand, a few approaches specialise in tracking multiple interacting hands [TTT*17, TBS*16] or interaction with objects [SMZ*16, TA18].

Face Tracking is important for social applications such as video conferencing and telepresence. Two recent surveys provide an up-to-date overview and evaluation of techniques for face reconstruction, tracking and applications [CAS*18, ZTG*18]. However, head-mounted near-eye displays create new challenges for face tracking because they occlude a large part of the face. Occlusion-aware techniques [HMYL15] partially address this problem, while other approaches integrate pressure sensors into the edge of the head-mounted display to directly measure the deformation of the face [LTO*15]. When combined with in-headset eye tracking, the reconstructed facial models become more expressive, which enables high-fidelity facial and speech animation [OLSL16] as well as gaze-aware facial reenactment [TZS*18].

Multimodal Tracking is an emerging area, which simultaneously tracks multiple modalities to obtain a more comprehensive reconstruction of the user. Such approaches for example combine tracking of bodies and hands [RTB17] or bodies, hands and faces [JSS18].

Environment Reconstruction is required to understand how a user interacts with the real world, and hence also the virtual world. Recent surveys provide an excellent introduction to and overview of 3D reconstruction using RGB-D cameras [ZSG*18], as well as simultaneous localisation and mapping (SLAM) in static [CCC*16] and dynamic environments [SMT18]. Most 3D reconstruction approaches assume static environments and integrate multiple depth maps from a moving camera using a truncated signed distance function, e.g. the pioneering KinectFusion approach [NDI*11]. Subsequent work expanded the supported capture volume using voxel hashing [NZIS13], added support for colour video cameras [PRI*13], achieved high performance on mobile devices [KPR*15], and integrated loop-closure optimisation with surface re-integration [DNZ*17]. More recent work goes beyond reconstructing just geometry and also estimates part labels to help understand real-world environments [XTZ15, DCS*17]. Most environments, however, are not entirely static and require non-rigid reconstruction and motion tracking [ZNI*14, NFS15], deformation of integration volumes [IZN*16], dense visual SLAM [WSMG*16] or L_0 motion regularisation [GXW*18].

4.3. Tracking Applications

In this section, we review a select set of tracking applications in VR/AR: gaze tracking to speed up rendering while maintaining visual fidelity, and gesture/gaze tracking to control user interfaces.

Gaze-Aware Displays Being able to detect and to adapt to the gaze direction facilitates many new ways to enhance digital displays. The notion of gaze-contingent or gaze-aware display devices dates back at least two decades. In the following, some of the most recent key contributions of the field are presented. Excellent review articles on gaze-contingent techniques and applications include those of Reingold [RLMS03], O'Sullivan [OHM*04], Duchowski [DCM04],

DÇ07], Dietrich [DG07], Bartz et al. [BCFW08], Masia et al. [MWDG13] and Stengel et al. [SM16].

Another application for eye tracking in HMDs is foveated rendering [GFD*12, SGEM16, PSK*16, WRK*16], which we briefly touched on in Section 3.3. The rapid fall-off in acuity from our foveal to our peripheral field of vision is exploited to allocate rendering and video processing resources more efficiently. Stengel et al. present a perception model for adaptive image-space sampling [SGEM16]. In this work, the scene is rendered and displayed in full detail only within a small circle around the gaze direction, and the rendered image resolution decreases continuously with increasing angular distance from the foveal field of vision. Weier et al. present a perception-based foveation scheme using ray tracing [WRK*16, WRHS18]. In recent work, Mauderer et al. created a model for simultaneous contrast perception [MFN16]. The approach modulates the colour of the scene in the periphery according to the gaze direction, which results in more saturated colour perception. The authors plan to use the effect to create a new form of high dynamic range images with increased perceivable gamut size [MFN16]. Patney et al. show that the level of foveation can be increased if the local contrast is boosted and therefore perceptually maintained [PSK*16]. In follow-up work, Sun et al. have presented foveation for light-field displays [SHK*17]. Lungaro et al. present a fast foveation scheme for reducing bandwidth requirements during video transmission [LSV*18].

Dedicated measurements to determine acceptable latency for gaze-contingent displays have been conducted in several studies [EMAH04, LW07, RJG*14, APLK17]. The measured *end-to-end latency* comprises the full gaze capture, rendering and display pipeline, starting with capturing the frame for eye-tracking and ending with the reception of the photons emitted by the display by the photoreceptors in the retina. Loschky et al. observed that the display has to be refreshed after 5 ms to 60 ms following a saccade for an image update to go undetected. The acceptable delay depends on the task of the application and the stimulus size in terms of induced peripheral degradation. Beyond that time delay, detection likelihood rises quickly [LW07]. It is therefore important to decide if the intended task is concerned with perceptual fidelity or visual performance. Albert et al. present latency requirements for a variety of VR scenarios [APLK17].

Under normal circumstances, attention is guided by visual features and the task of the user, which is exploited for passive gaze prediction [KDCM14]. Strategies for gaze guidance are aiming for steering attention to a specified target location, which can significantly differ from the natural fixation location. Therefore, gaze guidance requires altering the visible scene content. McNamara and Bailey introduced a more subtle, yet effective gaze guidance strategy [MBS*12, BMSG09]. The authors apply image-space modulations in the luminance channel to guide a viewer's gaze through a scene without interrupting their visual experience. The principle has been successfully applied to increase search task performance as well as to direct gaze in narrative art [MBS*12]. Hence, the technique may support understanding of a painting in a gallery or a related use case, but may also be useful for gaze guidance in simulators and training, pervasive advertising or perceptually adaptive rendering [BMSG09]. Grogorkick et al. explored subtle gaze

direction for wide field of view scenarios in immersive environments [GSEM17]. Recently, Sun et al. successfully apply subtle gaze guidance for redirected walking in VR [SPW*18]. Along similar lines, Langbehn et al. exploit blink-induced suppression for the same redirected walking task [LSL*18].

Gesture-Driven User Interfaces 3D gestural interaction provides an intuitive and natural way of 3D interaction, often providing a detailed representation of hands and fingers visualised in a 3D spatial context, while using a near-eye display [LaV13, KPL17]. Accurately recognising detailed 3D gestures, especially involving subtle finger movement is paramount, so that interaction appears seamless. One of the key devices for hands/finger recognition, which provides low-latency, immediate interaction with 3D space is the Leap Motion device. Because of its low cost, it became available to a wide range of users of entertainment as well as XR training applications [Car16, NLB14]. The Leap Motion is a small device connected via USB, which is often mounted onto a near-eye display. Using two monochromatic infrared (IR) cameras and three IR LEDs, the device recognises gestures within approximately 1 metre. The LEDs generate pattern-less IR light and the cameras capture at around 200 Hz, synthesising 3D position data for fast hand tracking. The smaller range of recognition and higher resolution of the device differentiates Leap Motion from the Kinect, which is more suitable for full-body tracking in a space the size of a room [GB18, TSSL15]. Although advances in gestural recognition hardware are rapid and 3D gesture interfaces are now widely adopted, the technologies are not yet stable, especially in relation to full-body motion capture so that the ecological validity of immersive experiences is guaranteed [VPK17].

Gaze-Driven User Interfaces Gaze-based interaction is intuitive and natural as tasks can be performed directly in the spatial context without having to search for an out-of-view keyboard or mouse [Duc18]. Past research as early as the 1980s investigated eye-tracking-based interfaces to interact with 2D user interfaces [HWM*89], as well as gaze input for people with disabilities [YF87]. Using gaze as an interaction metaphor for attentive user interfaces is intuitive for search tasks, but also turns out to be ambiguous and error-prone when being used for selecting or triggering commands [Jac91]. Special graphical user interfaces reduce ambiguities for gaze writing tasks, but have not been able to reach interaction bandwidths that are competitive to established input devices such as the keyboard [WRSD08, PT08, MHL13]. Under normal conditions, the eye is used to gain information about the environment, but not to trigger commands. However, different studies have shown the gain in task performance if gaze is combined with other modalities, such as touch or head gestures [SD12, MHP12]. Recently, gaze-based interaction has been employed for Locked-In Syndrome (LIS) patients combining eye movement and electroencephalogram (EEG) signals confirming or cancelling gaze-based actions [HLZ*16].

A common issue when using an eye-tracked interface as an input device is known as the 'Midas touch' problem. Eye movements are involuntary and accidental interface activation is frequent. Fixation time could last from 450 ms to 1 second when a gaze-based interface is initially used, but has been shown to become faster with

experience to around 300 ms in the case of gaze typing [MAŠ09]. Faster fixation times, however, when requested as part of a formal experimental design are stressful to the users. Speech recognition has been used in the past to signify an event as a solution to the Midas touch issue, requiring accurate synchronisation of gaze and speech data streams in order to be reliable [KTH*03].

Eye tracking has been utilised for interaction in near-eye displays, showing performance improvements compared to finger pointing [TJ00]. Recently, various companies incorporate eye tracking in novel near-eye displays, such as the FOVE and Magic Leap, or providing add-ons for near-eye displays such as for the Oculus Rift and HoloLens [vdMKS17]. Eye-tracked interfaces for immersive viewing, covering commonly operated actions of everyday computing such as mail composing and multimedia viewing, have demonstrated less typing errors while operating the eye-controlled interface compared to using the standard keyboard, while invoking stronger enjoyment and satisfaction associated with the eye-tracked 3D interface [SKM15]. The Midas touch issue in gaze-driven near-eye displays is dealt with by employing an additional mechanical input (switch) to signify a selection in the immersive environment [SKM15], or a method in which users perform a distinctive two-step gaze gesture for object selection [MGFY18]. Recent research explored natural gaze-based interaction techniques in immersive environments, such as eye-gaze selection based on eye gaze and inertial reticles, cluttered object selection that takes advantage of smooth pursuit, and head-gesture-based interaction relying on the vestibulo-ocular reflex [PLLB17]. Gaze-based interaction is shown to improve user experience and can demonstrate, in some cases, comparable performance to standard interaction techniques.

5. Future Work

In this section, we discuss the variety of open problems and research challenges that remain unsolved.

The Vergence–Accommodation Conflict is one of the most significant ergonomic issues related to viewer fatigue. The conflict is common for most young users of modern consumer-grade immersive near-eye displays, when viewing stereoscopic 3D content [KBB17]. The conflict is caused because the plane of focus (i.e., the screen) is fixed, whereas eye vergence movements occur continuously when fusing stereoscopic content [HGAB08]. For example, in a VR gaming scenario, when the player is in control of the view, fast-moving collisions with buildings or objects will result in excessive disparities which, for the vast majority of users, cause visual strain and jeopardise the quality of the overall gaming experience. Symptoms range from slight discomfort that can cause major eye strain to visually-induced dizziness, and lead to significantly reduced depth perception. The level of discomfort increases with the exposure time to 3D content which is not calibrated for comfortable viewing. High disparities force the eyes to rotate unnaturally in relation to each other.

Software-based solutions to the vergence–accommodation conflict include the stereo-grading process, i.e., altering the depth structure of a scene by drawing objects in a user's comfortable disparity range, also known as the *comfort zone* of the observer, have demonstrated enhanced viewing comfort [KDCM16, KDM*16]. Recent

stereo grading advances for 3D games improve perceived quality based on the available gaze information, applying localised disparity management, for objects predicted to be attended or on areas based on the current task [KDCM16]. Such approaches smoothly relocate the perceived depth of attended objects/areas into the comfort zone, maintaining a rich sense of depth. However, stereo-grading solutions are software-based and rather limited, suffering from local or global card-boarding effects, often modifying depth and speed of objects and are not suitable for truly real-time arbitrary disparity manipulations [OHB*11]. Recently, it has been shown that accommodation can be driven quite effectively when significant optical aberrations of the human eye are taken into account when rendering for VR, in particular using chromatic aberration [CLS*17]. A combination of optical solutions, eye tracking and rendering techniques are now driving the development of consumer-driven near-eye displays. These methods, based on the focus-adjustable-lens design that drives accommodation effectively, truly have the potential to resolve the vergence–accommodation conflict in the near future.

Gaze Tracking is a mandatory technology for many of the proposed display concepts and therefore has to become an industry standard. Along these lines, Khronos OpenXR [Khr18] has become the most promising attempt to establish low-latency eye tracking as an open and cross-platform standard in the virtual reality and mixed reality software ecosystem. Augmented reality glasses introduce additional constraints in terms of power consumption and physical size of the tracking hardware. Reaching this goal requires more research on mobile, small-scale, low-power, robust and accurate eye-tracking technology. Although attempts using multiple miniature cameras or photo diodes are promising [TSSB17, LLZ17], these approaches are not yet suitable for accurate tracking under arbitrary lighting conditions and longer periods of time. Gaze prediction methods [ATM*17, KDCM15] and other specialised signal filters can be expected to reduce latency issues or high sampling rates.

The tracking equipment shifting over time with respect to the head also usually introduces errors in gaze estimation. Eye location estimation from camera frames facilitates drift compensation, but usually requires high-resolution data and is therefore only viable for VR or desktop scenarios. Eye trackers within AR devices have to solve this problem in new ways and might require additional low-power sensors measuring the head pose with respect to the AR device. With the advent of broadly used gaze tracking, we can expect new applications enabled by the user's gaze [SGE*15] as well as new usages of gaze data. Games and VR experiences will greatly benefit from gaze information to enable enhanced user interfaces, more social interaction through eye contact [SWM*08] and reduced computation efforts in rendering [PSK*16, SGEM16]. Multimodal saliency and attention models [EZP*13] could greatly improve the accuracy of user behaviour understanding and related applications, such as for foveated rendering.

In addition, user customisation and automated device calibration, user profiling and user-friendly identification will be enabled when biometric eye data can be acquired on the fly [FD00]. However, security and privacy of the individual user has to be maintained to prevent identity theft. Recently, eye tracking for medical rehabilitation has been shown to be feasible [YWL*17, ŽHH*17], e.g., to cure lazy eyes by learning to see 3D in VR, and then in reality. Blink rate, pupil

size and saccade measurements allow for cognitive state, behaviour, fatigue and emotion analysis in real time [AAGW14, ZS82, SS00]. Each of these components constitutes a great research field by itself. What is missing is an efficient way to acquire ground-truth data for the development of machine-learning-based methods.

User and Environment Tracking are crucial for achieving convincing and immersive virtual and augmented reality experiences [BCL15]. Research in these areas has made great progress in recent years, as witnessed by the wealth of techniques and approaches surveyed in Section 4. However, tracking is far from a solved problem. In our opinion, the four main remaining challenges that need to be addressed are robustness, speed, efficiency and availability. (1) *Robustness* is needed for real-world applications that go beyond the proof-of-concept stage demonstrated by current research prototypes. (2) *Speed* is a necessity, as the user and their environment need to be tracked in real time with minimal latency and high update rate to avoid disorientation and discomfort. (3) *Efficiency* is required when tracking needs to be performed within the limited resources of stand-alone devices, including limited computation, memory and power budgets. (4) *Availability* of state-of-the-art tracking implementations is currently limited as most are proprietary; freely available and generously licensed open-source implementations will facilitate the development of a larger range of future display devices, as it lowers the barrier of entry into the market. It is worth noting that not all areas of tracking face all of these challenges. Head tracking, for example, is arguably solved sufficiently robustly, quickly and efficiently in state-of-the-art consumer-level VR and AR head-mounted displays, but these implementations are proprietary and, to the best of our knowledge, there are no comparable free solutions.

6. Conclusion

In this state-of-the-art report, we summarised the established and recent work in the area of near-eye displays and tracking technologies. We first covered relevant background such as optics and human visual perception, and then described the most fundamental but also the most recent advances in immersive near-eye display and tracking technologies. However, despite decades of research and progress, a variety of open problems and research challenges delineated in the previous section, such as the vergence–accommodation conflict and user and environment tracking, remain unsolved. One of the leading drivers of future headset innovations will be advancements in optics technology. Significant progress in focus-adjustable lens assemblies is expected to provide a much more comfortable HMD experience. In future headset designs it may also be necessary to measure accommodation *in situ*. Pivotal improvements in wavefront accommodation sensing such as the Hartmann-Shack sensor will allow the development of practical systems for widespread use.

We hope that our discussion of these challenges will inspire research on future directions needing further investigation. We look forward to these advances.

Acknowledgements C.R. acknowledges funding from RCUK grant CAMERA (EP/M023281/1) and an EPSRC-UKRI Innovation Fellowship (EP/S001050/1).

Appendix A: Acronyms

AMOLED	Active-Matrix Organic Light-Emitting Diode
AR	Augmented Reality
BFI	Black Frame Insertion
CBF	Circular Binary Features
CPD	Cycles Per Degree
CSF	Contrast Sensitivity Function
DoF	Degree of Freedom
EEG	Electroencephalogram
FoV	Field of View
HDR	High Dynamic Range
HMD	Head-Mounted Display
HOE	Holographic Optical Element
HVS	Human Visual System
IMU	Inertial Measurement Unit
IPD	Interpupillary Distance
IPS	In-Plane Switching
IR	Infrared
LCD	Liquid Crystal Display
LCoS	Liquid Crystal on Silicon
LED	Light Emitting Diode
LIS	Locked-In Syndrome
MAR	Minimum Angle of Resolution
MEMS	Micro-Electro-Mechanical Systems
MVA	Multidomain Vertical Alignment
NED	Near-Eye Display
NELD	Near-Eye Light-field Display
OLED	Organic Light Emitting Diode
SLAM	Simultaneous Localisation And Mapping
SLM	Spatial Light Modulator
SPEM	Smooth Pursuit Eye Motion
TN	Twisted Nematic
VAC	Vergence-Accommodation Conflict
VR	Virtual Reality
XR	Cross/Extended Reality

References

- [AAGW14] ALGHOWINEM S., ALSHEHRI M., GOECKE R., WAGNER M.: Exploring eye activity as an indication of emotional states using an eye-tracking sensor. In *Intelligent Systems for Science and Information*, Chen L., Kapoor S., Bhatia R., (Eds.). Springer, 2014, pp. 261–276. 18
- [ABG10] AMANO T., BIMBER O., GRUNDHÖFER A.: *Appearance Enhancement for Visually Impaired with Projector Camera Feedback*. Tech. rep., Bauhaus University Weimar, 2010. 11
- [ACR*19] AKŞIT K., CHAKRAVARTHULA P., RATHINAVEL K., JEONG Y., ALBERT R., FUCHS H., LUEBKE D.: Manufacturing application-driven foveated near-eye displays. *IEEE Trans. Vis. Comput. Graph.* (2019). 10
- [Ade82] ADELSON E. H.: Saturation and adaptation in the rod system. *Vision Research* 22, 10 (1982), 1299–1312. 4
- [AKGD17] ALVAREZ T. L., KIM E. H., GRANGER-DONETTI B.: Adaptation to progressive additive lenses: Potential factors to consider. *Scientific Reports* 7, 1 (2017), 2529. 10
- [AKL15] AKŞIT K., KAUTZ J., LUEBKE D.: Slim near-eye display using pinhole aperture arrays. *Applied Optics* 54, 11 (2015), 3422–3427. 9
- [ALK*17a] AKŞIT K., LOPES W., KIM J., SHIRLEY P., LUEBKE D.: Near-eye varifocal augmented reality display using see-through screens. *ACM Trans. Graph.* 36, 6 (2017), 189:1–13. 9, 10
- [ALK*17b] AKŞIT K., LOPES W., KIM J., SPJUT J., PATNEY A., SHIRLEY P., LUEBKE D., CHOLEWIAK S. A., SRINIVASAN P., NG R., BANKS M. S., LOVE G. D.: Varifocal virtuality: A novel optical layout for near-eye display. In *SIGGRAPH Emerging Technologies* (2017), pp. 25:1–2. 10
- [APLK17] ALBERT R., PATNEY A., LUEBKE D., KIM J.: Latency requirements for foveated rendering in virtual reality. *ACM Trans. Appl. Percept.* 14, 4 (2017), 25. 16
- [ARS*18] ALEXANDER J., ROUDAUT A., STEIMLE J., HORNBAEK K., BRUNS ALONSO M., FOLLMER S., MERRITT T.: Grand challenges in shape-changing interface research. In *CHI* (2018). 7
- [ATM*17] ARABADZHIYSKA E., TURSUN O. T., MYSZKOWSKI K., SEIDEL H.-P., DIDYK P.: Saccade landing position prediction for gaze-contingent rendering. *ACM Trans. Graph.* 36, 4 (2017), 50:1–12. 17
- [AWGB04] AKELEY K., WATT S. J., GIRSHICK A. R., BANKS M. S.: A stereo display prototype with multiple focal distances. *ACM Trans. Graph.* 23, 3 (2004), 804–813. 9
- [Bak49] BAKER H. D.: The course of foveal light adaptation measured by the threshold intensity increment. *J. Opt. Soc. Am.* 39, 2 (1949), 172–179. 4
- [Bal81] BALDWIN D.: Area of interest: Instantaneous field of view vision model. In *Image Generation/Display Conference* (1981), pp. 481–496. 10
- [Bar04] BARTEN P. G. J.: Formula for the contrast sensitivity of the human eye. In *Image Quality and System Performance* (2004), pp. 231–238. 3
- [BCFW08] BARTZ D., CUNNINGHAM D., FISCHER J., WALLRAVEN C.: The role of perception for computer graphics. In *Eurographics State-of-the-Art Reports* (2008), pp. 65–86. 16
- [BCL15] BILLINGHURST M., CLARK A., LEE G.: A survey of augmented reality. *Foundations and Trends in Human-Computer Interaction* 8, 2–3 (2015), 73–272. 12, 13, 18
- [BDF16] BAPAT A., DUNN E., FRAHM J. M.: Towards kilo-Hertz 6-DoF visual tracking using an egocentric cluster of rolling shutter cameras. *IEEE Trans. Vis. Comput. Graph.* 22, 11 (2016), 2358–2367. 13, 14
- [BKLP04] BOWMAN D., KRUIJFF E., LAVIOLA JR. J. J., POUPLYREV I. P.: *3D User interfaces: theory and practice, CourseSmart eTextbook*. Addison-Wesley, 2004. 7
- [BKV11] BOLTON J., KIM K., VERTEGAAL R.: SnowGlobe: A spherical fish-tank VR display. In *CHI Extended Abstracts* (2011), pp. 1159–1164. 7
- [BLW*17] BUCKNOR B., LOPEZ C., WOODS M. J., ALY A. H. M., PALMER J. W., RYNEK E. F.: Electromagnetic tracking with augmented reality systems. *US Patent Application US20170307891A1*, 2017. 12, 13
- [BMSG09] BAILEY R., MCNAMARA A., SUDARSANAM N., GRIMM C.: Subtle gaze direction. *ACM Trans. Graph.* 28, 4 (2009), 100:1–14. 16
- [BPH13] BROCKMEYER E., POUPLYREV I., HUDSON S.: PAPILLON: designing curved display surfaces with printed optics. In *UIST* (2013), pp. 457–462. 7
- [Bre56] BREWSTER D.: *The Stereoscope: Its History, Theory, and Construction*. John Murray, 1856. 8, 11
- [Bro99] BROOKS JR F. P.: What's real about virtual reality? *IEEE Comput. Graph. Appl.* 19, 6 (1999), 16–27. 1
- [BSA91] BANKS M. S., SEKULER A. B., ANDERSON S. J.: Peripheral spatial vision: Limits imposed by optics, photoreceptors, and receptor pooling. *J. Opt. Soc. Am.* 8, 11 (1991), 1775–1787. 3
- [BW10] BENKO H., WILSON A. D.: Multi-point interactions with immersive omnidirectional visualizations in a dome. In *International Conference on Interactive Tabletops and Surfaces (ITS)* (2010), pp. 19–28. 7
- [BWB08] BENKO H., WILSON A. D., BALAKRISHNAN R.: Sphere: Multi-touch interactions on a spherical display. In *UIST* (2008), pp. 77–86. 7
- [Car16] CARDOSO J. C. S.: Comparison of gesture, gamepad, and gaze-based locomotion for VR worlds. In *VRST* (2016), pp. 319–320. 16
- [CAS*18] CHRYSOS G. G., ANTONAKOS E., SNAPE P., ASTHANA A., ZAFEIRIOU S.: A comprehensive performance evaluation of deformable face tracking “in-the-wild”. *Int. J. Comput. Vision* 126, 2 (2018), 198–232. 15
- [CCC*16] CADENA C., CARLONE L., CARRILLO H., LATIF Y., SCARAMUZZA D., NEIRA J., REID I., LEONARD J. J.: Past, present, and future of simultaneous localization and mapping: Toward the robust-perception age. *IEEE Transactions on Robotics* 32, 6 (2016), 1309–1332. 13, 15
- [CDAF18] CHAKRAVARTHULA P., DUNN D., AKŞIT K., FUCHS H.: FocusAR: Auto-focus augmented reality eyeglasses for both real world and virtual imagery. *IEEE Trans. Vis. Comput. Graph.* 24, 11 (2018), 2906–2916. 11
- [CKS18] CHANG J.-H. R., KUMAR B. V. K. V., SANKARANARAYANAN A. C.: Towards multifocal displays with dense focal stacks. *ACM Trans. Graph.* 37, 6 (2018), 198:1–17. 9
- [CLS*17] CHOLEWIAK S. A., LOVE G. S., SRINIVASAN P. P., NG R., BANKS M. S.: ChromaBlur: Rendering chromatic eye aberration improves accommodation and realism. *ACM Trans. Graph.* 36, 6 (2017), 210:1–12. 17
- [CLvdHE16] CUPERUS A. A., LAKEN M., VAN DEN HOUT M. A., ENGELHARD I. M.: Degrading emotional memories induced by a virtual reality paradigm. *J. Behav. Ther. Exp. Psychiatry* 52 (2016), 45–50. 8
- [CR06] ÇAKMAKCI O., ROLLAND J.: Head-worn displays: a review. *J. Disp. Technol.* 2, 3 (2006), 199–216. 9, 10
- [CSKH90] CURCIO C. A., SLOAN K. R., KALINA R. E., HENDRICKSON A. E.: Human photoreceptor topography. *J. Comp. Neurol.* 292, 4 (1990), 497–523. 2, 3
- [CV95] CUTTING J. E., VISHTON P. M.: Perceiving layout and knowing distances: The integration, relative potency, and contextual use of different information about depth. In *Perception of Space and Motion*, Epstein W., Rogers S., (Eds.). Academic Press, 1995, pp. 69–117. 2
- [CWHT09] CHENG D., WANG Y., HUA H., TALHA M.: Design of an optical see-through head-mounted display with a low f-number and large field of view using a freeform prism. *Applied Optics* 48, 14 (2009), 2655–2668. 9
- [DC07] DUCHOWSKI A. T., ÇÖLTEKIN A.: Foveated gaze-contingent displays for peripheral LOD management, 3D visualization, and stereo imaging. *ACM Trans. Multimed. Comput. Commun. Appl.* 3, 4 (2007), 6:1–18. 15

- [DCM04] DUCHOWSKI A. T., COURNIA N., MURPHY H.: Gaze-contingent displays: A review. *CyberPsychology & Behavior* 7, 6 (2004), 621–634. 15
- [DCS*17] DAI A., CHANG A. X., SAVVA M., HALBER M., FUNKHOUSER T., NIESSNER M.: ScanNet: Richly-annotated 3D reconstructions of indoor scenes. In *CVPR (2017)*, pp. 5828–5839. 14, 15
- [DDF*17] DOU M., DAVIDSON P., FANELLO S. R., KHAMIS S., KOWDLE A., RHEMANN C., TANKOVICH V., IZADI S.: Motion2Fusion: Real-time volumetric performance capture. *ACM Trans. Graph.* 36, 6 (2017), 246:1–16. 15
- [DF04] D'ANDRADE B. W., FORREST S. R.: White organic light-emitting devices for solid-state lighting. *Advanced Materials* 16, 18 (2004), 1585–1595. 5
- [DGY07] DIETRICH A., GOBBETTI E., YOON S.-E.: Massive-model rendering techniques: A tutorial. *IEEE Comput. Graph. Appl.* 27, 6 (2007), 20–34. 16
- [DH02] DIFEDE J., HOFFMAN H. G.: Virtual reality exposure therapy for World Trade Center post-traumatic stress disorder: A case report. *CyberPsychology & Behavior* 5, 6 (2002), 529–535. 7
- [DM64] DONDERS F. C., MOORE W. D.: *On the anomalies of accommodation and refraction of the eye: With a preliminary essay on physiological dioptries*, vol. 22. New Sydenham Society, 1864. 11
- [DNZ*17] DAI A., NIESSNER M., ZOLLHÖFER M., IZADI S., THEOBALT C.: BundleFusion: Real-time globally consistent 3D reconstruction using on-the-fly surface reintegration. *ACM Trans. Graph.* 36, 3 (2017), 24:1–18. 13, 15
- [DR90] DROESSLER J. G., ROTIER D. J.: Tilted cat helmet-mounted display. *Optical Engineering* 29, 8 (1990). 9
- [DTT*17] DUNN D., TIPPETS C., TORELL K., KELLNHOFFER P., AKŞIT K., DIDYK P., MYSZKOWSKI K., LUEBKE D., FUCHS H.: Wide field of view varifocal near-eye display using see-through deformable membrane mirrors. *IEEE Trans. Vis. Comput. Graph.* 23, 4 (2017), 1322–1331. 9, 10
- [Duc17] DUCHOWSKI A. T.: *Eye Tracking Methodology*, 3rd ed. Springer, 2017. 14
- [Duc18] DUCHOWSKI A. T.: Gaze-based interaction: A 30 year retrospective. *Computers & Graphics* 73 (2018), 59–69. 16
- [DXCZ15] DALY S., XU N., CRENSHAW J., ZUNJARAO V. J.: A psychophysical study exploring judder using fundamental signals and complex imagery. *SMPT Motion Imaging Journal* 124, 7 (2015), 62–70. 6
- [EKC18] ENGEL J., KOLTUN V., CREMERS D.: Direct sparse odometry. *IEEE Trans. Pattern Anal. Mach. Intell.* 40, 3 (2018), 611–625. 13
- [Ell94] ELLIS S. R.: What are virtual environments? *IEEE Comput. Graph. Appl.* 14, 1 (1994), 17–22. 1
- [EMAH04] ELLIS S. R., MANIA K., ADELSTEIN B. D., HILL M. I.: Generalizability of latency detection in a variety of virtual environments. *Proceedings of the Human Factors and Ergonomics Society Annual Meeting* 48, 23 (2004), 2632–2636. 16
- [ESS*16] EBSTYNE M. J., SCHAFFALITZKY F., STEEDLY D., CHAN C., EADE E., KIPMAN A., KLEIN G.: Pose tracking an augmented reality device. *US Patent 9495801B2*, 2016. 13
- [EZP*13] EVANGELOPOULOS G., ZLATINTSI A., POTAMIANOS A., MARAGOS P., RAPANTZIKOS K., SKOUMAS G., AVRITHIS Y.: Multimodal saliency and fusion for movie summarization based on aural, visual, and textual attention. *IEEE Transactions on Multimedia* 15, 7 (2013), 1553–1568. 17
- [FD00] FRISCHHOLZ R. W., DIECKMANN U.: Biold: a multimodal biometric identification system. *Computer* 33, 2 (2000), 64–68. 17
- [Fen06] FENG X.-F.: LCD motion-blur analysis, perception, and reduction using synchronized backlight flashing. In *Human Vision and Electronic Imaging* (2006). 7
- [FGS*18] FUHL W., GEISLER D., SANTINI T., APPEL T., ROSENSTIEL W., KASNECI E.: CBF: Circular binary features for robust and real-time pupil center detection. In *ETRA (2018)*, pp. 8:1–6. 14
- [FKS*15] FUHL W., KÜBLER T., SIPPEL K., ROSENSTIEL W., KASNECI E.: ExCuSe: Robust pupil detection in real-world scenarios. In *International Conference on Computer Analysis of Images and Patterns* (2015), pp. 39–51. 14
- [FR84] FISCHER B., RAMSPERGER E.: Human express saccades: extremely short reaction times of goal directed eye movements. *Experimental Brain Research* 57, 1 (1984), 191–195. 4
- [Fry39] FRY G. A.: Further experiments on the accommodation-convergence relationship. *Optometry and Vision Science* 16, 9 (1939), 325–336. 11
- [FSKK16] FUHL W., SANTINI T. C., KÜBLER T., KASNECI E.: Ellipse selection for robust pupil detection in real-world environments. In *ETRA (2016)*, pp. 123–130. 14
- [GB18] GONÇALVES A., BERMÚDEZ S.: KAVE: Building Kinect based CAVE automatic virtual environments, methods for surround-screen projection management, motion parallax and full-body interaction support. *Proc. ACM Hum.-Comput. Interact.* 2, EICS (2018), 10. 16
- [GFD*12] GUENTER B., FINCH M., DRUCKER S., TAN D., SNYDER J.: Foveated 3D graphics. *ACM Trans. Graph.* 31, 6 (2012), 164:1–10. 16
- [GHM*06] GELINCK G. H., HUITEMA H. E. A., MIL M., VEENENDAAL E., LIESHOUT P. J. G., TOWSLAGER F., PATRY S. F., SOHN S., WHITESIDES T., MCCREARY M. D.: A rollable, organic electrophoretic qvga display with field-shielded pixel architecture. *Journal of the Society for Information Display* 14, 2 (2006), 113–118. 7
- [Gil91] GILBOA P.: Designing the right visor. In *Large Screen Projection, Avionic, and Helmet-Mounted Displays* (1991). 9
- [GMB06] GODIN G., MASSICOTTE P., BORGEAT L.: High-resolution insets in projector-based stereoscopic displays: principles and techniques. In *Stereoscopic Displays and Virtual Reality Systems* (2006). 10
- [Gol10a] GOLDSTEIN E. B.: *Encyclopedia of perception*. SAGE Publications, Inc, 2010. 2, 4
- [Gol10b] GOLDSTEIN E. B.: *Sensation and Perception*, 8th ed. Wadsworth-Thomson Learning, Pacific Grove, 2010. 2, 3
- [Goo17] GOODMAN J. W.: *Introduction to Fourier optics*, 4th ed. W. H. Freeman, 2017. 5
- [GSEM17] GROGORICK S., STENDEL M., EISEMANN E., MAGNOR M.: Subtle gaze guidance for immersive environments. In *Symposium on Applied Perception* (2017), pp. 4:1–7. 16
- [GWW*16] GOU C., WU Y., WANG K., WANG F.-Y., JI Q.: Learning-by-synthesis for accurate eye detection. In *ICPR (2016)*, pp. 3362–3367. 14
- [GXW*18] GUO K., XU F., WANG Y., LIU Y., DAI Q.: Robust non-rigid motion tracking and surface reconstruction using L_0 regularization. *IEEE Trans. Vis. Comput. Graph.* 24, 5 (2018). 14, 15
- [HB16] HAINICH R. R., BIMBER O.: *Displays: Fundamentals & Applications*, 2nd ed. A K Peters/CRC Press, 2016. 5, 6
- [HCOB10] HELD R. T., COOPER E. A., O'BRIEN J. F., BANKS M. S.: Using blur to affect perceived distance and size. *ACM Trans. Graph.* 29, 2 (2010), 19:1–16. 2
- [HCW15] HUANG F.-C., CHEN K., WETZSTEIN G.: The light field stereoscope: Immersive computer graphics via factored near-eye light field displays with focus cues. *ACM Trans. Graph.* 34, 4 (2015), 60:1–12. 9
- [HFU13] HEDILI M. K., FREEMAN M. O., UREY H.: Microlens array-based high-gain screen design for direct projection head-up displays. *Applied Optics* 52, 6 (2013), 1351–1357. 7
- [HGAB08] HOFFMAN D. M., GIRSHICK A. R., AKELEY K., BANKS M. S.: Vergence–accommodation conflicts hinder visual performance and cause visual fatigue. *Journal of Vision* 8, 3 (2008), 33. 8, 17

- [HH91] HORTON J., HOYT W.: The representation of the visual field in human striate cortex. a revision of the classic Holmes map. *Archives of Ophthalmology* 109, 6 (1991), 816–824. 4
- [HH14] HU X., HUA H.: High-resolution optical see-through multi-focal-plane head-mounted display using freeform optics. *Optics Express* 22, 11 (2014), 13896–13903. 9, 10
- [HJ14] HUA H., JAVIDI B.: A 3D integral imaging optical see-through head-mounted display. *Optics Express* 22, 11 (2014), 13484–13491. 10
- [HKMA07] HÖLLERER T., KUCHERA-MORIN J., AMATRIAIN X.: The Allosphere: A large-scale immersive surround-view instrument. In *Workshop on Emerging Displays Technologies* (2007). 7
- [HKN*16] HUANG M. X., KWOK T. C., NGAI G., CHAN S. C., LEONG H. V.: Building a personalized, auto-calibrating eye tracker from user interactions. In *CHI* (2016), pp. 5169–5179. 14
- [HLNL17] HUANG M. X., LI J., NGAI G., LEONG H. V.: ScreenGlint: Practical, in-situ gaze estimation on smartphones. In *CHI* (2017), pp. 2546–2557. 15
- [HLZ*16] HAN S., LIU R., ZHU C., SOO Y. G., YU H., LIU T., DUAN F.: Development of a human computer interaction system based on multi-modal gaze tracking methods. In *International Conference on Robotics and Biomimetics* (2016), pp. 1894–1899. 16
- [HMYL15] HSIEH P.-L., MA C., YU J., LI H.: Unconstrained realtime facial performance capture. In *CVPR* (2015), pp. 1675–1683. 15
- [HNA*11] HOLMQUIST K., NYSTRÖM M., ANDERSSON R., DEWHURST R., JARODZKA H., VAN DE WEIJER J.: *Eye tracking: A comprehensive guide to methods and measures*. OUP Oxford, 2011. 14
- [How92] HOWLETT E. M.: High-resolution inserts in wide-angle head-mounted stereoscopic displays. In *Stereoscopic Displays and Applications* (1992), pp. 193–204. 10
- [How12] HOWARD I. P. (Ed.): *Perceiving in Depth, Volume 1: Basic Mechanisms*. Oxford University Press, 2012. 4
- [HPG09] HANSEN T., PRACEJUS L., GEGENFURTNER K. R.: Color perception in the intermediate periphery of the visual field. *Journal of Vision* 9, 4 (2009), 26:1–12. 3
- [HR95] HOWARD I. P., ROGERS B. J.: *Binocular vision and stereopsis*. Oxford University Press, 1995. 2
- [HS14] HALE K. S., STANNEY K. M. (Eds.): *Handbook of virtual environments: Design, implementation, and applications, 2nd ed.* CRC Press, 2014. 7
- [Hua17] HUA H.: Enabling focus cues in head-mounted displays. *Proc. IEEE* 105, 5 (2017), 805–824. 8, 9
- [HWBR14] HUANG F.-C., WETZSTEIN G., BARSKY B. A., RASKAR R.: Eyeglasses-free display: Towards correcting visual aberrations with computational light field displays. *ACM Trans. Graph.* 33, 4 (2014), 59:1–12. 11
- [HWC*17] HSU C.-H., WU Y.-L., CHENG W.-H., CHEN Y.-J., HUA K.-L.: HoloTube: a low-cost portable 360-degree interactive autostereoscopic display. *Multimedia Tools and Applications* 76, 7 (2017), 9099–9132. 7
- [HWM*89] HUTCHINSON T. E., WHITE K. P., MARTIN W. N., REICHERT K. C., FREY L. A.: Human-computer interaction using eye-gaze input. *IEEE Transactions on Systems, Man, and Cybernetics* 19, 6 (1989), 1527–1534. 16
- [HZQ*14] HSU C. W., ZHEN B., QIU W., SHAPIRA O., DELACY B. G., JOANNPOULOS J. D., SOLJAČIĆ M.: Transparent displays enabled by resonant nanoparticle scattering. *Nature Communications* 5 (2014). 7
- [IAIK16] ITOH Y., AMANO T., IWAI D., KLINKER G.: Gaussian light field: Estimation of viewpoint-dependent blur for optical see-through head-mounted displays. *IEEE Trans. Vis. Comput. Graph.* 22, 11 (2016), 2368–2376. 11
- [IK15] ITOH Y., KLINKER G.: Vision enhancement: Defocus correction via optical see-through head-mounted displays. In *Augmented Human International Conference* (2015), pp. 1–8. 11
- [IZN*16] INNEMANN M., ZOLLHÖFER M., NIESSNER M., THEOBALT C., STAMMINGER M.: VolumeDeform: Real-time volumetric non-rigid reconstruction. In *ECCV* (2016). 14, 15
- [Jac91] JACOB R. J. K.: The use of eye movements in human-computer interaction techniques: What you look at is what you get. *ACM Trans. Inf. Syst.* 9, 2 (1991), 152–169. 16
- [JBM*17] JANG C., BANG K., MOON S., KIM J., LEE S., LEE B.: Retinal 3D: Augmented reality near-eye display via pupil-tracked light field projection on retina. *ACM Trans. Graph.* 36, 6 (2017), 190:1–13. 10
- [Jer09] JERALD J. J.: *Scene-Motion- and Latency-Perception Thresholds for Head-Mounted Displays*. PhD thesis, University of North Carolina at Chapel Hill, 2009. 12
- [JHB*15] JAVADI A.-H., HAKIMI Z., BARATI M., WALSH V., TCHEANG L.: SET: a pupil detection method using sinusoidal approximation. *Frontiers in Neuroengineering* 8 (2015). 14
- [JPK*16] JOHNSON P. V., PARNELL J. A. Q., KIM J., SAUNTER C. D., BANKS M. S., LOVE G. D.: Assessing visual discomfort using dynamic lens and monovision displays. In *Imaging and Applied Optics* (2016), p. TT4A.1. 8
- [JSS18] JOO H., SIMON T., SHEIKH Y.: Total capture: A 3D deformation model for tracking faces, hands, and bodies. In *CVPR* (2018). 15
- [JW95] JOHNSTON R. S., WILLEY S. R.: Development of a commercial retinal scanning display. In *Helmet- and Head-Mounted Displays and Symbology Design Requirements* (1995), pp. 2–14. 9
- [KAB18] KHAMIS M., ALT F., BULLING A.: The past, present, and future of gaze-enabled handheld mobile devices: Survey and lessons learned. In *MobileHCI* (2018), pp. 38:1–17. 14
- [KB99] KATO H., BILLINGHURST M.: Marker tracking and HMD calibration for a video-based augmented reality conferencing system. In *International Workshop on Augmented Reality* (1999), pp. 85–94. 13
- [KBBD17] KOULIERIS G. A., BUI B., BANKS M. S., DRETTAKIS G.: Accommodation and comfort in head-mounted displays. *ACM Trans. Graph.* 36, 4 (2017), 87:1–11. 8, 9, 17
- [KBKL10] KOLB A., BARTH E., KOCH R., LARSEN R.: Time-of-flight cameras in computer graphics. *Comput. Graph. Forum* 29, 1 (2010), 141–159. 13
- [KC17] KAR A., CORCORAN P.: A review and analysis of eye-gaze estimation systems, algorithms and performance evaluation methods in consumer platforms. *IEEE Access* 5 (2017), 16495–16519. 14
- [KCW16] KONRAD R., COOPER E. A., WETZSTEIN G.: Novel optical configurations for virtual reality: Evaluating user preference and performance with focus-tunable and monovision near-eye displays. In *CHI* (2016), pp. 1211–1220. 9
- [KDCM14] KOULIERIS G. A., DRETTAKIS G., CUNNINGHAM D., MANIA K.: C-LOD: Context-aware material level-of-detail applied to mobile graphics. *Comput. Graph. Forum* 33, 4 (2014), 41–49. 16
- [KDCM15] KOULIERIS G. A., DRETTAKIS G., CUNNINGHAM D., MANIA K.: An automated high-level saliency predictor for smart game balancing. *ACM Trans. Appl. Percept.* 11, 4 (2015), 17:1–21. 4, 17
- [KDCM16] KOULIERIS G. A., DRETTAKIS G., CUNNINGHAM D., MANIA K.: Gaze prediction using machine learning for dynamic stereo manipulation in games. In *IEEE VR* (2016), pp. 113–120. 17
- [KDM*16] KELLNHOFFER P., DIDYK P., MYSZKOWSKI K., HEFEEDA M. M., SEIDEL H.-P., MATUSIK W.: GazeStereo3D: Seamless disparity manipulations. *ACM Trans. Graph.* 35, 4 (2016), 68:1–13. 17
- [KFSW09] KIENZLE W., FRANZ M. O., SCHÖLKOPF B., WICHMANN F. A.: Center-surround patterns emerge as optimal predictors for human saccade targets. *Journal of Vision* 9, 5 (2009), 7:1–15. 4
- [KHI*12] KIM D., HILLIGES O., IZADI S., BUTLER A. D., CHEN J., OIKONOMIDIS I., OLIVIER P.: Digits: Freehand 3D interactions anywhere using a wrist-worn gloveless sensor. In *UIST* (2012), pp. 167–176. 15

- [Khr18] KHRONOS GROUP: OpenXR. [GDC Presentation](#), 2018. 17
- [KK17] KOTARU M., KATTI S.: Position tracking for virtual reality using commodity WiFi. In *CVPR (2017)*, pp. 2671–2681. 12
- [KKK*14] KISHISHITA N., KIYOKAWA K., KRUIJFF E., ORLOSKY J., MASHITA T., TAKEMURA H.: Analysing the effects of a wide field of view augmented reality display on search performance in divided attention tasks. In *ISMAR (2014)*, pp. 177–186. 4
- [KKK*16] KRAFKA K., KHOSLA A., KELLNHOFER P., KANNAN H., BHANDARKAR S., MATUSIK W., TORRALBA A.: Eye tracking for everyone. In *CVPR (2016)*, pp. 2176–2184. 14
- [KLT*09] KOLB A., LAMBERS M., TODT S., CUNTZ N., REZK-SALAMA C.: Immersive rear projection on curved screens. In *IEEE VR (2009)*, pp. 285–286. 7
- [KM15] KUMAR P., MAES P.: Penetra3D: A penetrable, interactive, 360-degree viewable display. In *3DUI (2015)*, pp. 169–170. 7
- [Kow11] KOWLER E.: Eye movements: The past 25 years. *Vision Research* 51, 13 (2011), 1457–1483. 4
- [KPB14] KASSNER M., PATERA W., BULLING A.: Pupil: an open source platform for pervasive eye tracking and mobile gaze-based interaction. In *UbiComp Adjunct Publication (2014)*, pp. 1151–1160. 14
- [KPL17] KULSHRESHTH A., PFEIL K., LAVIOLA JR. J. J.: Enhancing the gaming experience using 3D spatial user interface technologies. *IEEE Comput. Graph. Appl.* 37, 3 (2017), 16–23. 16
- [KPR*15] KÄHLER O., PRISACARIU V. A., REN C. Y., SUN X., TORR P., MURRAY D.: Very high frame rate volumetric integration of depth images on mobile devices. *IEEE Trans. Vis. Comput. Graph.* 21, 11 (2015), 1241–1250. 15
- [Kra16] KRAMIDA G.: Resolving the vergence-accommodation conflict in head-mounted displays. *IEEE Trans. Vis. Comput. Graph.* 22, 7 (2016), 1912–1931. 9
- [KS13a] KRESS B., SHIN M.: Diffractive and holographic optics as optical combiners in head mounted displays. In *UbiComp Adjunct Publication (2013)*, pp. 1479–1482. 9
- [KS13b] KRESS B., STARNER T.: A review of head-mounted displays (HMD) technologies and applications for consumer electronics. In *Photonic Applications for Aerospace, Commercial, and Harsh Environments (2013)*. 8
- [KSH*17] KIM J., SUN Q., HUANG F.-C., WEI L.-Y., LUEBKE D., KAUFMAN A.: Perceptual studies for foveated light field displays. [arXiv:1708.06034](#), 2017. 10
- [KSM*19] KIM J., STENDEL M., MAJERCIC A., DE MELLO S., LAINE S., MCGUIRE M., LUEBKE D.: NVGaze: An anatomically-informed dataset for low-latency, near-eye gaze estimation. In *CHI (2019)*. 14, 15
- [KTH*03] KAUR M., TREMAINE M., HUANG N., WILDER J., GACOVSKI Z., FLIPPO F., MANTRAVADI C. S.: Where is “it”? Event synchronization in gaze-speech input systems. In *International Conference on Multimodal Interfaces (2003)*, pp. 151–158. 17
- [LaV13] LAVIOLA JR. J. J.: 3D gestural interaction: The state of the field. *ISRN Artificial Intelligence 2013 (2013)*, 514641. 16
- [LCH08] LIU S., CHENG D., HUA H.: An optical see-through head mounted display with addressable focal planes. In *ISMAR (2008)*, pp. 33–42. 9, 10
- [LCL*18] LEE S., CHO J., LEE B., JO Y., JANG C., KIM D., LEE B.: Foveated retinal optimization for see-through near-eye multi-layer displays. *IEEE Access* 6 (2018), 2170–2180. 9, 10
- [LFOI15] LEITHINGER D., FOLLMER S., OLWAL A., ISHII H.: Shape displays: Spatial interaction with dynamic physical form. *IEEE Comput. Graphics Appl.* 35, 5 (2015), 5–11. 7
- [LHG*18] LAFFONT P.-Y., HASNAIN A., GUILLEMET P.-Y., WIRAJAYA S., KHOO J., TENG D., BAZIN J.-C.: Verifocal: a platform for vision correction and accommodation in head-mounted displays. In *SIGGRAPH Emerging Technologies (2018)*, pp. 21:1–2. 11
- [LJY*18] LEE S., JO Y., YOO D., CHO J., LEE D., LEE B.: TomoReal: Tomographic displays. [arXiv:1804.04619](#), 2018. 9
- [LK18] LANDER C., KRÜGER A.: EyeSense: Towards information extraction on corneal images. In *Adjunct Proceedings of UbiComp/ISWC (2018)*, pp. 980–987. 15
- [LKKC17] LEE S. M., KWON J. H., KWON S., CHOI K. C.: A review of flexible OLEDs toward highly durable unusual displays. *IEEE Trans. Electron Devices* 64, 5 (2017), 1922–1931. 7
- [LL13] LANMAN D., LUEBKE D.: Near-eye light field displays. *ACM Trans. Graph.* 32, 6 (2013), 220:1–10. 9
- [LLB*15] LEUTENEGGER S., LYNEN S., BOSSE M., SIEGWART R., FURGALE P.: Keyframe-based visual–inertial odometry using nonlinear optimization. *The International Journal of Robotics Research* 34, 3 (2015), 314–334. 13
- [LLJ*16] LI G., LEE D., JEONG Y., CHO J., LEE B.: Holographic display for see-through augmented reality using mirror-lens holographic optical element. *Optics Letters* 41, 11 (2016), 2486–2489. 9
- [LLZ17] LI T., LIU Q., ZHOU X.: Ultra-low power gaze tracking for virtual reality. In *Conference on Embedded Network Sensor Systems (2017)*, pp. 25:1–14. 17
- [LN07] LINDEMAN R. W., NOMA H.: A classification scheme for multi-sensory augmented reality. In *VRST (2007)*, pp. 175–178. 4
- [LNH*11] LEVIN L., NILSSON S., HOEVE J. V., WU S., KAUFMAN P., ALM A.: *Adler’s Physiology of the Eye*, 11th ed. Elsevier, 2011. 2, 3, 4
- [LSC04] LEDDA P., SANTOS L. P., CHALMERS A.: A local model of eye adaptation for high dynamic range images. In *AFRIGRAPH (2004)*, pp. 151–160. 4
- [LSL*18] LANGBEHN E., STEINICKE F., LAPPE M., WELCH G. F., BRUDER G.: In the blink of an eye: Leveraging blink-induced suppression for imperceptible position and orientation redirection in virtual reality. *ACM Trans. Graph.* 37, 4 (2018), 66:1–11. 16
- [LSV*18] LUNGARO P., SJÖBERG R., VALERO A. J. F., MITTAL A., TOLLMAR K.: Gaze-aware streaming solutions for the next generation of mobile VR experiences. *IEEE Trans. Vis. Comput. Graph.* 24, 4 (2018), 1535–1544. 16
- [LSZ*18] LANGLOTZ T., SUTTON J., ZOLLMANN S., ITOH Y., REGENBRECHT H.: ChromaGlasses: Computational-glasses for compensating colour blindness. In *CHI (2018)*, pp. 390:1–12. 11
- [LTO*15] LI H., TRUTOIU L., OLSZEWSKI K., WEI L., TRUTNA T., HSIEH P.-L., NICHOLLS A., MA C.: Facial performance sensing head-mounted display. *ACM Trans. Graph.* 34, 4 (2015), 47:1–9. 14, 15
- [Luc06] LUCKE R. L.: Rayleigh-Sommerfeld Fraunhofer diffraction. [arXiv:physics/0604229](#), 2006. 5
- [LW07] LOSCHKY L. C., WOLVERTON G. S.: How late can you update gaze-contingent multiresolutional displays without detection? *ACM Trans. Multimedia Comput. Commun. Appl.* 3, 4 (2007), 7:1–10. 16
- [LWP05] LI D., WINFIELD D., PARKHURST D. J.: Starburst: A hybrid algorithm for video-based eye tracking combining feature-based and model-based approaches. In *CVPR Workshops (2005)*, p. 79. 14
- [LYKA14] LAVALLE S. M., YERSHOVA A., KATSEV M., ANTONOV M.: Head tracking for the Oculus Rift. In *ICRA (2014)*, pp. 187–194. 12, 13
- [MAŠ09] MAJARANTA P., AHOLA U.-K., ŠPAKOV O.: Fast gaze typing with an adjustable dwell time. In *CHI (2009)*, pp. 357–360. 17
- [MBS*12] MCNAMARA A., BOOTH T., SRIDHARAN S., CAFFEY S., GRIMM C., BAILEY R.: Directing gaze in narrative art. In *Symposium on Applied Perception (2012)*, pp. 63–70. 16
- [MBS*18] MUELLER F., BERNARD F., SOTNYCHENKO O., MEHTA D., SRIDHAR S., CASAS D., THEOBALT C.: GANerated hands for real-time 3D hand tracking from monocular RGB. In *CVPR (2018)*. 15

- [MBW*17] MARIAKAKIS A., BAUDIN J., WHITMIRE E., MEHTA V., BANKS M. A., LAW A., MCGRATH L., PATEL S. N.: PupilScreen: Using smartphones to assess traumatic brain injury. *Proc. ACM Interact. Mob. Wearable Ubiquitous Technol.* 1, 3 (2017), 81:1–27. 14, 15
- [MCNV14] MAUDERER M., CONTE S., NACENTA M. A., VISHWANATH D.: Depth perception with gaze-contingent depth of field. In *CHI* (2014), pp. 217–226. 10
- [MDMS05] MANTIUK R., DALY S. J., MYSZKOWSKI K., SEIDEL H.-P.: Predicting visible differences in high dynamic range images: model and its calibration. In *Human Vision and Electronic Imaging* (2005), pp. 204–215. 6
- [MFL17] MATSUDA N., FIX A., LANMAN D.: Focal surface displays. *ACM Trans. Graph.* 36, 4 (2017), 86:1–86:14. 10
- [MFN16] MAUDERER M., FLATLA D. R., NACENTA M. A.: Gaze-contingent manipulation of color perception. In *CHI* (2016), pp. 5191–5202. 16
- [MGDA*15] MONTALTO C., GARCIA-DORADO I., ALIAGA D., OLIVEIRA M. M., MENG F.: A total variation approach for customizing imagery to improve visual acuity. *ACM Trans. Graph.* 34, 3 (2015), 28:1–16. 11
- [MGFY18] MOHAN P., GOH W. B., FU C.-W., YEUNG S.-K.: Dual-Gaze: Addressing the Midas touch problem in gaze mediated VR interaction. In *Adjunct Proceedings of ISMAR* (2018). 17
- [MGK17] MAIMONE A., GEORGIU A., KOLLIN J. S.: Holographic near-eye displays for virtual and augmented reality. *ACM Trans. Graph.* 36, 4 (2017), 85:1–16. 9, 10
- [MHKS11] MOESLUND T. B., HILTON A., KRÜGER V., SIGAL L. (Eds.): *Visual Analysis of Humans: Looking at People*. Springer, 2011. 15
- [MHL13] MÖLLENBACH E., HANSEN J. P., LILLHOLM M.: Eye movements in gaze interaction. *Journal of Eye Movement Research* 6, 2 (2013), 16
- [MHP12] MARDANBEGI D., HANSEN D. W., PEDERSON T.: Eye-based head gestures. In *ETRA* (2012), pp. 139–146. 16
- [MLR*14] MAIMONE A., LANMAN D., RATHINAVEL K., KELLER K., LUEBKE D., FUCHS H.: Pinlight displays: Wide field of view augmented reality eyeglasses using defocused point light sources. *ACM Trans. Graph.* 33, 4 (2014), 89:1–11. 10
- [MMS15] MANTIUK R. K., MYSZKOWSKI K., SEIDEL H.-P.: High dynamic range imaging. In *Wiley Encyclopedia of Electrical and Electronics Engineering*. Wiley, 2015, pp. 1–42. 6
- [MMS*17] MUELLER F., MEHTA D., SOTNYCHENKO O., SRIDHAR S., CASAS D., THEOBALT C.: Real-time hand tracking under occlusion from an egocentric RGB-D sensor. In *ICCV* (2017), pp. 1163–1172. 14, 15
- [MN15] MATSUNAGA S., NAYAR S. K.: Field curvature correction using focal sweep. *IEEE Trans. Comput. Imaging* 1, 4 (2015), 259–269. 11
- [MS08] MORENO I., SUN C.-C.: Modeling the radiation pattern of LEDs. *Optics Express* 16, 3 (2008), 1808–1819. 5
- [MSM*17] MERCIER O., SULAI Y., MACKENZIE K., ZANNOLI M., HILLIS J., NOWROUZEZAHRAI D., LANMAN D.: Fast gaze-contingent optimal decompositions for multifocal displays. *ACM Trans. Graph.* 36, 6 (2017), 237:1–15. 9
- [MSS*17] MEHTA D., SRIDHAR S., SOTNYCHENKO O., RHODIN H., SHAFIEI M., SEIDEL H.-P., XU W., CASAS D., THEOBALT C.: VNect: Real-time 3D human pose estimation with a single RGB camera. *ACM Trans. Graph.* 36, 4 (2017), 44:1–14. 14, 15
- [Mul85] MULLEN K. T.: The contrast sensitivity of human colour vision to red-green and blue-yellow chromatic gratings. *The Journal of Physiology* 359, 1 (1985), 381–400. 3
- [MUS16] MARCHAND E., UCHIYAMA H., SPINDLER F.: Pose estimation for augmented reality: A hands-on survey. *IEEE Trans. Vis. Comput. Graph.* 22, 12 (2016), 2633–2651. 12, 13
- [MWDG13] MASIA B., WETZSTEIN G., DIDYK P., GUTIERREZ D.: A survey on computational displays: Pushing the boundaries of optics, computation, and perception. *Computers & Graphics* 37, 8 (2013), 1012–1038. 16
- [NAB*15] NARAIN R., ALBERT R. A., BULBUL A., WARD G. J., BANKS M. S., O'BRIEN J. F.: Optimal presentation of imagery with focus cues on multi-plane displays. *ACM Trans. Graph.* 34, 4 (2015), 59:1–12. 9
- [NDI*11] NEWCOMBE R. A., DAVISON A. J., IZADI S., KOHLI P., HILLIGES O., SHOTTON J., MOLYNEAUX D., HODGES S., KIM D., FITZGIBBON A.: KinectFusion: Real-time dense surface mapping and tracking. In *ISMAR* (2011), pp. 127–136. 14, 15
- [NFS15] NEWCOMBE R. A., FOX D., SEITZ S. M.: DynamicFusion: Reconstruction and tracking of non-rigid scenes in real-time. In *CVPR* (2015), pp. 343–352. 15
- [NKOE83] NOORLANDER C., KOENDERINK J. J., OLDEN R. J. D., EDENS B. W.: Sensitivity to spatiotemporal colour contrast in the peripheral visual field. *Vision Research* 23, 1 (1983), 1–11. 3
- [NLB14] NABIYOUNI M., LAHA B., BOWMAN D. A.: Designing effective travel techniques with bare-hand interaction. In *3DUI Posters* (2014), pp. 139–140. 16
- [NZIS13] NIESSNER M., ZOLLHÖFER M., IZADI S., STAMMINGER M.: Real-time 3D reconstruction at scale using voxel hashing. *ACM Trans. Graph.* 32, 6 (2013), 169:1–11. 15
- [OHB*11] OSKAM T., HORNING A., BOWLES H., MITCHELL K., GROSS M.: OSCAM – optimized stereoscopic camera control for interactive 3D. *ACM Trans. Graph.* 30, 6 (2011), 189:1–8. 17
- [OHM*04] O'SULLIVAN C., HOWLETT S., MORVAN Y., McDONNELL R., O'CONNOR K.: Perceptually adaptive graphics. In *Eurographics State-of-the-Art Reports* (2004). 15
- [OKA11] OIKONOMIDIS I., KYRIAZIS N., ARGYROS A.: Efficient model-based 3D tracking of hand articulations using Kinect. In *BMVC* (2011), pp. 101.1–11. 15
- [OLSL16] OLSZEWSKI K., LIM J. J., SAITO S., LI H.: High-fidelity facial and speech animation for VR HMDs. *ACM Trans. Graph.* 35, 6 (2016), 221:1–14. 15
- [OWS14] OLBERDING S., WESSELY M., STEIMLE J.: PrintScreen: Fabricating highly customizable thin-film touch-displays. In *UIST* (2014), pp. 281–290. 7
- [Pai05] PAI D. K.: Multisensory interaction: Real and virtual. In *International Symposium on Robotics Research* (2005), pp. 489–498. 4
- [Pal99] PALMER S. E.: *Vision Science: Photons to Phenomenology*. MIT Press, 1999. 2, 5, 6
- [PB71] POSNER M. I., BOIES S. J.: Components of attention. *Psychological Review* 78, 5 (1971), 391–408. 4
- [PDSH17] PENG Y., DUN X., SUN Q., HEIDRICH W.: Mix-and-match holography. *ACM Trans. Graph.* 36, 6 (2017), 191:1–12. 6
- [PKW18] PADMANABAN N., KONRAD R., WETZSTEIN G.: Autofocals: gaze-contingent eyeglasses for presbyopes. In *SIGGRAPH Emerging Technologies* (2018), pp. 3:1–2. 11
- [Pla13] PLANCK M.: *The theory of heat radiation*. Courier Corporation, 2013. 5
- [PLLB17] PIUMSOMBOON T., LEE G., LINDEMAN R. W., BILLINGHURST M.: Exploring natural eye-gaze-based interaction for immersive virtual reality. In *3DUI* (2017), pp. 36–39. 17
- [PN02] PARKHURST D. J., NIEBUR E.: Variable-resolution displays: A theoretical, practical, and behavioral evaluation. *Human Factors* 44, 4 (2002), 611. 10
- [PR98] PRINCE S. J., ROGERS B. J.: Sensitivity to disparity corrugations in peripheral vision. *Vision Research* 38, 17 (1998), 2533–2537. 4

- [PRI*13] PRADEEP V., RHEMANN C., IZADI S., ZACH C., BLEYER M., BATHICHE S.: MonoFusion: Real-time 3D reconstruction of small scenes with a single web camera. *In ISMAR (2013)*, pp. 83–88. 15
- [PSH18] PARK S., SPURR A., HILLIGES O.: Deep pictorial gaze estimation. *In ECCV (2018)*. 14
- [PSK*16] PATNEY A., SALVI M., KIM J., KAPLANYAN A., WYMAN C., BENTY N., LUEBKE D., LEFOHN A.: Towards foveated rendering for gaze-tracked virtual reality. *ACM Trans. Graph.* 35, 6 (2016), 179:1–12. 10, 16, 17
- [PT08] PORTA M., TURINA M.: Eye-S: a full-screen input modality for pure eye-based communication. *In ETRA (2008)*, pp. 27–34. 16
- [PZBH18] PARK S., ZHANG X., BULLING A., HILLIGES O.: Learning to find eye region landmarks for remote gaze estimation in unconstrained settings. *In ETRA (2018)*, pp. 21:1–10. 14
- [Rat65] RATLIFF F.: *Mach bands: quantitative studies on neural networks*. Holden-Day, 1965. 6
- [RBSJ79] RAAB F. H., BLOOD E. B., STEINER T. O., JONES H. R.: Magnetic position and orientation tracking system. *IEEE Trans. Aerosp. Electron. Syst.* 15, 5 (1979), 709–718. 12
- [RCR18] RUIZ N., CHONG E., REHG J. M.: Fine-grained head pose estimation without keypoints. *In CVPR Workshops (2018)*. 13, 14
- [Red73] REDER S. M.: On-line monitoring of eye-position signals in contingent and noncontingent paradigms. *Behavior Research Methods & Instrumentation* 5, 2 (1973), 218–228. 10
- [RF00] ROLLAND J. P., FUCHS H.: Optical versus video see-through head-mounted displays in medical visualization. *Presence: Teleoperators and Virtual Environments* 9, 3 (2000). 8
- [RJG*14] RINGER R. V., JOHNSON A. P., GASPAR J. G., NEIDER M. B., CROWELL J., KRAMER A. F., LOSCHKY L. C.: Creating a new dynamic measure of the useful field of view using gaze-contingent displays. *In ETRA (2014)*, pp. 59–66. 16
- [RKS*14] ROGEZ G., KHADEMI M., SUPANČIĆ III J. S., MONTIEL J. M. M., RAMANAN D.: 3D hand pose detection in egocentric RGB-D images. *In ECCV Workshops (2014)*, pp. 356–371. 15
- [RLMS03] REINGOLD E. M., LOSCHKY L. C., MCCONKIE G. W., STAMPE D. M.: Gaze-contingent multiresolutional displays: An integrative review. *Human Factors* 45, 2 (2003), 307–328. 15
- [RMGB01] ROSS J., MORRONE M., GOLDBERG M. E., BURR D. C.: Changes in visual perception at the time of saccades. *Trends in Neurosciences* 24, 2 (2001), 113–121. 4
- [Rot89] ROTIER D. J.: Optical approaches to the helmet mounted display. *In Helmet-Mounted Displays (1989)*. 9
- [RPPH12] RASMUSSEN M. K., PEDERSEN E. W., PETERSEN M. G., HORNBEK K.: Shape-changing interfaces: A review of the design space and open research questions. *In CHI (2012)*, pp. 735–744. 7
- [RRC*16] RHODIN H., RICHARDT C., CASAS D., INSAFUTDINOV E., SHAFIEI M., SEIDEL H.-P., SCHIELE B., THEOBALT C.: EgoCap: Egocentric marker-less motion capture with two fisheye cameras. *ACM Trans. Graph.* 35, 6 (2016), 162:1–11. 14, 15
- [RTB*16] ROLLAND J. P., THOMPSON K. P., BAUER A., UREY H., THOMAS M.: See-through head-worn display (hwd) architectures. *In Handbook of Visual Display Technology*, Chen J., Cranton W., Fihn M., (Eds.). Springer, 2016, pp. 2929–2961. 9
- [RTB17] ROMERO J., TZIONAS D., BLACK M. J.: Embodied hands: Modeling and capturing hands and bodies together. *ACM Trans. Graph.* 36, 6 (2017), 245:1–17. 14, 15
- [RVN78] ROVAMO J., VIRSU V., NÄSÄNEN R.: Cortical magnification factor predicts the photopic contrast sensitivity of peripheral vision. *Nature* 271, 5640 (1978), 54–56. 3
- [RYDR98] ROLLAND J. P., YOSHIDA A., DAVIS L. D., REIF J. H.: High-resolution inset head-mounted display. *Applied Optics* 37, 19 (1998), 4183–4193. 10
- [SAP*16] SHIN J., AN G., PARK J.-S., BAEK S. J., LEE K.: Application of precise indoor position tracking to immersive virtual reality with translational movement support. *Multimedia Tools and Applications* 75, 20 (2016), 12331–12350. 12, 13
- [SB15] SUGANO Y., BULLING A.: Self-calibrating head-mounted eye trackers using egocentric visual saliency. *In UIST (2015)*, pp. 363–372. 13, 14
- [SC18] SHERMAN W. R., CRAIG A. B.: *Understanding Virtual Reality: Interface, Application, and Design*, 2nd ed. Morgan Kaufmann, 2018. 11
- [SD12] STELLMACH S., DACHSELT R.: Look & touch: gaze-supported target acquisition. *In CHI (2012)*, pp. 2981–2990. 16
- [SD14] ŚWIRSKI L., DODGSON N. A.: Rendering synthetic ground truth images for eye tracker evaluation. *In ETRA (2014)*, pp. 219–222. 14
- [SDP*18] SITZMANN V., DIAMOND S., PENG Y., DUN X., BOYD S., HEIDRICH W., HEIDE F., WETZSTEIN G.: End-to-end optimization of optics and image processing for achromatic extended depth of field and super-resolution imaging. *ACM Trans. Graph.* 37, 4 (2018), 114:1–13. 6
- [SFK17] SANTINI T., FUHL W., KASNECI E.: CalibMe: Fast and unsupervised eye tracker calibration for gaze-based pervasive human-computer interaction. *In CHI (2017)*, pp. 2594–2605. 15
- [SFK18] SANTINI T., FUHL W., KASNECI E.: PuRe: Robust pupil detection for real-time pervasive eye tracking. *Comput. Vision Image Understanding* 170 (2018), 40–50. 14
- [SGE*15] STENDEL M., GROGORICK S., EISEMANN M., EISEMANN E., MAGNOR M. A.: An affordable solution for binocular eye tracking and calibration in head-mounted displays. *In International Conference on Multimedia (2015)*, pp. 15–24. 17
- [SGEM16] STENDEL M., GROGORICK S., EISEMANN M., MAGNOR M.: Adaptive image-space sampling for gaze-contingent real-time rendering. *Comput. Graph. Forum* 35, 4 (2016), 129–139. 16, 17
- [SGF*13] SHOTTON J., GIRSHICK R., FITZGIBBON A., SHARP T., COOK M., FINOCCHIO M., MOORE R., KOHLI P., CRIMINISI A., KIPMAN A., BLAKE A.: Efficient human pose estimation from single depth images. *IEEE Trans. Pattern Anal. Mach. Intell.* 35, 12 (2013), 2821–2840. 15
- [Sha49] SHANNON C. E.: Communication in the presence of noise. *Proceedings of the Institute of Radio Engineers* 37, 1 (1949), 10–21. 2
- [She87] SHENKER M.: Optical design criteria for binocular helmet-mounted displays. *In Display System Optics (1987)*, pp. 70–79. 10
- [SHK*17] SUN Q., HUANG F.-C., KIM J., WEI L.-Y., LUEBKE D., KAUFMAN A.: Perceptually-guided foveation for light field displays. *ACM Trans. Graph.* 36, 6 (2017), 192:1–13. 16
- [SHL*17] SHI L., HUANG F.-C., LOPES W., MATUSIK W., LUEBKE D.: Near-eye light field holographic rendering with spherical waves for wide field of view interactive 3D computer graphics. *ACM Trans. Graph.* 36, 6 (2017), 236:1–17. 10
- [SK07] SMITH E. E., KOSSLYN S. M.: *Cognitive Psychology: Mind and Brain*, 1 ed. Pearson/Prentice Hall, 2007. 4, 5
- [SKM15] SIDORAKIS N., KOUlieris G. A., MANIA K.: Binocular eye-tracking for the control of a 3D immersive multimedia user interface. *In Workshop on Everyday Virtual Reality (2015)*, pp. 15–18. 17
- [SM16] STENDEL M., MAGNOR M.: Gaze-contingent computational displays: Boosting perceptual fidelity. *IEEE Signal Processing Magazine* 33, 5 (2016), 139–148. 10, 16
- [SMOT15] SRIDHAR S., MUELLER F., OULASVIRTA A., THEOBALT C.: Fast and robust hand tracking using detection-guided optimization. *In CVPR (2015)*, pp. 3213–3221. 15
- [SMS14] SUGANO Y., MATSUSHITA Y., SATO Y.: Learning-by-synthesis for appearance-based 3D gaze estimation. *In CVPR (2014)*, pp. 1821–1828. 14
- [SMT18] SAPUTRA M. R. U., MARKHAM A., TRIGONI N.: Visual SLAM and structure from motion in dynamic environments: A survey. *ACM Computing Surveys* 51, 2 (2018), 37:1–36. 13, 15

- [SMZ*16] SRIDHAR S., MUELLER F., ZOLLHÖFER M., CASAS D., OULASVIRTA A., THEOBALT C.: Real-time joint tracking of a hand manipulating an object from RGB-D input. In *ECCV* (2016). 15
- [Spo82] SPOONER A. M.: *The trend towards area of interest in visual simulation technology*. Tech. rep., Naval Training Equipment Center, 1982. 10
- [SPS*11] SHIRATORI T., PARK H. S., SIGAL L., SHEIKH Y., HODGINS J. K.: Motion capture from body-mounted cameras. *ACM Trans. Graph.* 30, 4 (2011), 31:1–10. 15
- [SPW*18] SUN Q., PATNEY A., WEI L.-Y., SHAPIRA O., LU J., ASENTE P., ZHU S., MCGUIRE M., LUEBKE D., KAUFMAN A.: Towards virtual reality infinite walking: dynamic saccadic redirection. *ACM Trans. Graph.* 37, 4 (2018), 67:1–13. 16
- [SS00] SIREVAAG E. J., STERN J. A.: Ocular measures of fatigue and cognitive factors. *Engineering psychophysiology: Issues and applications* (2000), 269–287. 18
- [SS01] SHIMOJO S., SHAMS L.: Sensory modalities are not separate modalities: plasticity and interactions. *Current Opinion in Neurobiology* 11, 4 (2001), 505–509. 4
- [SS03] SPENCE C., SQUIRE S.: Multisensory integration: Maintaining the perception of synchrony. *Current Biology* 13, 13 (2003), 519–521. 4
- [SU16] SOOMRO S. R., UREY H.: Design, fabrication and characterization of transparent retro-reflective screen. *Optics Express* 24, 21 (2016), 24232–24241. 7
- [Sut68] SUTHERLAND I. E.: A head-mounted three dimensional display. In *Fall Joint Computer Conference* (1968), pp. 757–764. 9, 12, 13
- [Sut02] SUTCLIFFE A.: *Multimedia and Virtual Reality: Designing Usable Multisensory User Interfaces*. L. Erlbaum Associates Inc., 2002. 4
- [SWM*08] STEPTOE W., WOLFF R., MURGIA A., GUIMARAES E., RAE J., SHARKEY P., ROBERTS D., STEED A.: Eye-tracking for avatar eye-gaze and interactional analysis in immersive collaborative virtual environments. In *Conference on Computer Supported Cooperative Work* (2008), pp. 197–200. 17
- [SZ15] SIMONYAN K., ZISSERMAN A.: Very deep convolutional networks for large-scale image recognition. In *Proceedings of the International Conference on Learning Representations (ICLR)* (2015). 15
- [TA18] TSOLI A., ARGYROS A. A.: Joint 3D tracking of a deformable object in interaction with a hand. In *ECCV* (2018), pp. 484–500. 15
- [TBC*16] TAYLOR J., BORDEAUX L., CASHMAN T., CORISH B., KESKIN C., SHARP T., SOTO E., SWEENEY D., VALENTIN J., LUFF B., TOPALIAN A., WOOD E., KHAMIS S., KOHLI P., IZADI S., BANKS R., FITZGIBBON A., SHOTTON J.: Efficient and precise interactive hand tracking through joint, continuous optimization of pose and correspondences. *ACM Trans. Graph.* 35, 4 (2016), 143:1–12. 15
- [TBS*16] TZIONAS D., BALLAN L., SRIKANTHA A., APONTE P., POLLEFEYS M., GALL J.: Capturing hands in action using discriminative salient points and physics simulation. *Int. J. Comput. Vision* 118, 2 (2016), 172–193. 15
- [TdAS*10] THEOBALT C., DE AGUIAR E., STOLL C., SEIDEL H.-P., THRUN S.: Performance capture from multi-view video. In *Image and Geometry Processing for 3-D Cinematography*, Ronfard R., Taubin G., (Eds.), vol. 5. Springer, 2010, pp. 127–149. 15
- [TFCRS16] THOMPSON W., FLEMING R., CREEM-REGEHR S., STEFANUCCI J. K.: *Visual perception from a computer graphics perspective*. AK Peters/CRC Press, 2016. 6
- [TG80] TREISMAN A. M., GELADE G.: A feature-integration theory of attention. *Cognitive Psychology* 12, 1 (1980), 97–136. 5
- [TGFTB01] THORPE S., GEGENFURTNER K., FABRE-THORPE M., BÜLTHOFF H.: Detection of animals in natural images using far peripheral vision. *European Journal of Neuroscience* 14, 5 (2001), 869–876. 4
- [TJ00] TANRIVERDI V., JACOB R. J. K.: Interacting with eye movements in virtual environments. In *CHI* (2000), pp. 265–272. 17
- [TNSMP17] TOKUDA Y., NORASIKIN M. A., SUBRAMANIAN S., MARTINEZ PLASENCIA D.: MistForm: Adaptive shape changing fog screens. In *CHI* (2017), pp. 4383–4395. 7
- [TPT16] TKACH A., PAULY M., TAGLIASACCHI A.: Sphere-meshes for real-time hand modeling and tracking. *ACM Trans. Graph.* 35, 6 (2016), 222:1–11. 15
- [TSSB17] TONSEN M., STEIL J., SUGANO Y., BULLING A.: InvisibleEye: Mobile eye tracking using multiple low-resolution cameras and learning-based gaze estimation. *Proc. ACM Interact. Mob. Wearable Ubiquitous Technol.* 1, 3 (2017), 106:1–21. 15, 17
- [TSSL15] TARANTA II E. M., SIMONS T. K., SUKTHANKAR R., LAVIOLA JR. J. J.: Exploring the benefits of context in 3D gesture recognition for game-based virtual environments. *ACM Trans. Interact. Intell. Syst.* 5, 1 (2015), 1:1–34. 16
- [TTN18] TAN D. J., TOMBARI F., NAVAB N.: Real-time accurate 3D head tracking and pose estimation with consumer RGB-D cameras. *Int. J. Comput. Vision* 126, 2–4 (2018), 158–183. 13
- [TTT*17] TAYLOR J., TANKOVICH V., TANG D., KESKIN C., KIM D., DAVIDSON P., KOWDLE A., IZADI S.: Articulated distance fields for ultra-fast tracking of hands interacting. *ACM Trans. Graph.* 36, 6 (2017), 244:1–12. 14, 15
- [TZS*18] THIES J., ZOLLHÖFER M., STAMMINGER M., THEOBALT C., NIESSNER M.: FaceVR: Real-time gaze-aware facial reenactment in virtual reality. *ACM Trans. Graph.* 37, 2 (2018), 25:1–15. 14, 15
- [vdMKS17] VAN DER MEULEN H., KUN A. L., SHAER O.: What are we missing?: Adding eye-tracking to the HoloLens to improve gaze estimation accuracy. In *International Conference on Interactive Surfaces and Spaces* (2017), pp. 396–400. 17
- [vKP10] VAN KREVELEN D. W. F., POELMAN R.: A survey of augmented reality technologies, applications and limitations. *International Journal of Virtual Reality* 9, 2 (2010), 1–20. 7
- [VMGM15] VANGORP P., MYRSKOWSKI K., GRAF E. W., MANTIUK R. K.: A model of local adaptation. *ACM Trans. Graph.* 34, 6 (2015), 166:1–13. 4
- [VPK17] VASYLEVSKA K., PODKOSOVA I., KAUFMANN H.: Teaching virtual reality with HTC Vive and Leap Motion. In *SIGGRAPH Asia Symposium on Education* (2017), pp. 2:1–8. 16
- [VRWM78] VOLKMAN F. C., RIGGS L. A., WHITE K. D., MOORE R. K.: Contrast sensitivity during saccadic eye movements. *Vision Research* 18, 9 (1978), 1193–1199. 4
- [Wan95] WANDELL B. A.: *Foundations of Vision*. Stanford University, 1995. 2, 3
- [WB97] WOLFE J. M., BENNETT S. C.: Preattentive object files: Shapeless bundles of basic features. *Vision Research* 37, 1 (1997), 25–43. 4
- [WBM*16] WOOD E., BALTRUŠAITIS T., MORENCY L.-P., ROBINSON P., BULLING A.: Learning an appearance-based gaze estimator from one million synthesised images. In *ETRA* (2016), pp. 131–138. 14
- [WBZ*15] WOOD E., BALTRUŠAITIS T., ZHANG X., SUGANO Y., ROBINSON P., BULLING A.: Rendering of eyes for eye-shape registration and gaze estimation. In *ICCV* (2015), pp. 3756–3764. 14, 15
- [WC97] WICKENS C. D., CARSWELL C. M.: *Information Processing*. John Wiley & Sons, Inc., 1997, pp. 130–149. 5
- [WDK93] WOODS A. J., DOCHERTY T., KOCH R.: Image distortions in stereoscopic video systems. In *Stereoscopic Displays and Applications* (1993). 8
- [WDW99] WILLIAMS A. M., DAVIDS K., WILLIAMS J. G. P.: *Visual Perception & Action in Sport*. Taylor & Francis, 1999. 4
- [WF02] WELCH G., FOXLIN E.: Motion tracking: no silver bullet, but a respectable arsenal. *IEEE Comput. Graph. Appl.* 22, 6 (2002), 24–38. 12, 13

- [WHL10] WETZSTEIN G., HEIDRICH W., LUEBKE D.: Optical image processing using light modulation displays. *Comput. Graph. Forum* 29, 6 (2010), 1934–1944. 11
- [WLX16] WANG J., LIANG Y., XU M.: Design of a see-through head-mounted display with a freeform surface. *Journal of the Optical Society of Korea* 19, 6 (2016), 614–618. 9
- [WP04] WEISENBERGER J. M., POLING G. L.: Multisensory roughness perception of virtual surfaces: effects of correlated cues. In *International Symposium on Haptic Interfaces for Virtual Environment and Teleoperator Systems* (2004), pp. 161–168. 4
- [WPDH14] WANG R. I., PELFREY B., DUCHOWSKI A. T., HOUSE D. H.: Online 3D gaze localization on stereoscopic displays. *ACM Trans. Appl. Percept.* 11, 1 (2014), 3:1–21. 13, 14
- [WRHS18] WEIER M., ROTH T., HINKENJANN A., SLUSALLEK P.: Foveated depth-of-field filtering in head-mounted displays. *ACM Trans. Appl. Percept.* 15, 4 (2018), 26:1–14. 16
- [WRK*16] WEIER M., ROTH T., KRUIFF E., HINKENJANN A., PÉRARD-GAYOT A., SLUSALLEK P., LI Y.: Foveated real-time ray tracing for head-mounted displays. *Comput. Graph. Forum* 35, 7 (2016), 289–298. 16
- [WRSD08] WOBROCK J. O., RUBINSTEIN J., SAWYER M. W., DUCHOWSKI A. T.: Longitudinal evaluation of discrete consecutive gaze gestures for text entry. In *ETRA* (2008), pp. 11–18. 16
- [WSMG*16] WHELAN T., SALAS-MORENO R. F., GLOCKER B., DAVIDSON A. J., LEUTENEGGER S.: ElasticFusion: Real-time dense SLAM and light source estimation. *The International Journal of Robotics Research* 35, 14 (2016), 1697–1716. 15
- [WSR*17] WEIER M., STENDEL M., ROTH T., DIDYK P., EISEMANN E., EISEMANN M., GROGORICK S., HINKENJANN A., KRUIFF E., MAGNOR M., MYSKOWSKI K., SLUSALLEK P.: Perception-driven accelerated rendering. *Comput. Graph. Forum* 36, 2 (2017), 611–643. 2
- [WVSB10] WEISS M., VOELKER S., SUTTER C., BORCHERS J.: Bend-Desk: Dragging across the curve. In *International Conference on Interactive Tabletops and Surfaces* (2010), pp. 1–10. 7
- [WZC12] WEI X., ZHANG P., CHAI J.: Accurate realtime full-body motion capture using a single depth camera. *ACM Trans. Graph.* 31, 6 (2012), 188:1–12. 15
- [XCZ*18] XU W., CHATTERJEE A., ZOLLHÖFER M., RHODIN H., MEHTA D., SEIDEL H.-P., THEOBALT C.: MonoPerfCap: Human performance capture from monocular video. *ACM Trans. Graph.* 37, 2 (2018), 27:1–15. 14, 15
- [XCZ*19] XU W., CHATTERJEE A., ZOLLHÖFER M., RHODIN H., FUA P., SEIDEL H.-P., THEOBALT C.: Mo2Cap2: Real-time mobile 3D motion capture with a cap-mounted fisheye camera. *IEEE Trans. Vis. Comput. Graph.* (2019). 15
- [Yel83] YELLOTT J.: Spectral consequences of photoreceptor sampling in the rhesus retina. *Science* 221, 4608 (1983), 382–385. 3
- [YF87] YAMADA M., FUKUDA T.: Eye word processor (EWP) and peripheral controller for the ALS patient. *IEE Proceedings A* 134, 4 (1987), 328–330. 16
- [YFF07] YOUNG H. D., FREEDMAN R. A., FORD L.: *University Physics Vol. 2 (Chapters 21–37)*, vol. 2. Pearson education, 2007. 5
- [YJK*10] YOO J. S., JUNG S. H., KIM Y. C., BYUN S. C., KIM J. M., CHOI N. B., YOON S. Y., KIM C. D., HWANG Y. K., CHUNG I. J.: Highly flexible AM-OLED display with integrated gate driver using amorphous silicon TFT on ultrathin metal foil. *Journal of Display Technology* 6, 11 (2010), 565–570. 7
- [YS16] YATES A., SELAN J.: Positional tracking systems and methods. *US Patent Application US20160131761A1*, 2016. 13
- [YWL*17] YOW A. P., WONG D., LIU H., ZHU H., ONG I. J.-W., LAUDE A., LIM T. H.: Automatic visual impairment detection system for age-related eye diseases through gaze analysis. In *International Conference of the Engineering in Medicine and Biology Society* (2017), pp. 2450–2453. 17
- [YYN*16] YAMAMOTO A., YANAI Y., NAGAI M., SUZUKI R., ITO Y.: 16-3: A novel transparent screen using cholesteric liquid crystal dots. *Digest of Technical Papers* 47, 1 (2016), 185–188. 7
- [Zha12] ZHANG Z.: Microsoft Kinect sensor and its effect. *IEEE Multi-Media* 19, 2 (2012), 4–10. 13
- [ŽHH*17] ŽIAK P., HOLM A., HALIČKA J., MOJŽIŠ P., PIÑERO D. P.: Amblyopia treatment of adults with dichoptic training using the virtual reality Oculus Rift head mounted display: preliminary results. *BMC Ophthalmology* 17, 1 (2017), 105. 17
- [ZHSB18] ZHANG X., HUANG M. X., SUGANO Y., BULLING A.: Training person-specific gaze estimators from user interactions with multiple devices. In *CHI* (2018), pp. 624:1–12. 15
- [ZLAA*18] ZHAO M., LI T., ABU ALSHEIKH M., TIAN Y., ZHAO H., TORRALBA A., KATABI D.: Through-wall human pose estimation using radio signals. In *CVPR* (2018), pp. 7356–7365. 12
- [ZLW18] ZHAN T., LEE Y.-H., WU S.-T.: High-resolution additive light field near-eye display by switchable Pancharatnam–Berry phase lenses. *Optics Express* 26, 4 (2018), 4863–4872. 9
- [ZNI*14] ZOLLHÖFER M., NIESSNER M., IZADI S., RHEMANN C., ZACH C., FISHER M., WU C., FITZGIBBON A., LOOP C., THEOBALT C., STAMMINGER M.: Real-time non-rigid reconstruction using an RGB-D camera. *ACM Trans. Graph.* 33, 4 (2014), 156:1–12. 15
- [ZS82] ZANGEMEISTER W. H., STARK L.: Gaze latency: variable interactions of head and eye latency. *Experimental Neurology* 75, 2 (1982), 389–406. 18
- [ZSFB15] ZHANG X., SUGANO Y., FRITZ M., BULLING A.: Appearance-based gaze estimation in the wild. In *CVPR* (2015), pp. 4511–4520. 15
- [ZSFB19] ZHANG X., SUGANO Y., FRITZ M., BULLING A.: MPIIGaze: Real-world dataset and deep appearance-based gaze estimation. *IEEE Trans. Pattern Anal. Mach. Intell.* 41, 1 (2019), 162–175. 13, 15
- [ZSG*18] ZOLLHÖFER M., STOTKO P., GÖRLITZ A., THEOBALT C., NIESSNER M., KLEIN R., KOLB A.: State of the art on 3D reconstruction with RGB-D cameras. *Comput. Graph. Forum* 37, 2 (2018), 625–652. 15
- [ZTG*18] ZOLLHÖFER M., THIES J., GARRIDO P., BRADLEY D., BEELER T., PÉREZ P., STAMMINGER M., NIESSNER M., THEOBALT C.: State of the art on monocular 3D face reconstruction, tracking, and applications. *Comput. Graph. Forum* 37, 2 (2018), 523–550. 15
- [ZXTZ15] ZHANG Y., XU W., TONG Y., ZHOU K.: Online structure analysis for real-time indoor scene reconstruction. *ACM Trans. Graph.* 34, 5 (2015), 159:1–13. 15
- [ZZP*18] ZHOU X., ZHU M., PAVLAKOS G., LEONARDOS S., DERPANIS K. G., DANIILIDIS K.: MonoCap: Monocular human motion capture using a CNN coupled with a geometric prior. *IEEE Trans. Pattern Anal. Mach. Intell. preprints* (2018). 15

Author Biographies



Kaan Akşit is a senior research scientist at Nvidia Corporation located at Santa Clara, US, tackling the problems related to computational displays for virtual and augmented reality applications. He received his B.S. degree in electrical engineering from Istanbul Technical University, Turkey, his M.Sc. degree in electrical power engineering from RWTH Aachen University, Germany, and his Ph.D. degree in electrical engineering at Koç University, Turkey. In 2009, he joined Philips Research at Eindhoven, the Netherlands as an intern. In 2013, he joined Disney Research, Zurich, Switzerland as an intern. His past research includes topics such as visible light communications, optical medical sensing, solar cars, and auto-stereoscopic displays.



George Alex Koulieris is an Assistant Professor in the Innovative Computing Group, Dept. of Computer Science, Durham University, UK. Previously he was a post-doctoral researcher at Inria, France, and a visiting scholar at UC Berkeley, USA. He obtained his PhD from the Department of Electronic & Computer Engineering, TUC, Greece. He has designed display/optics hardware to investigate the effectiveness of methods that alleviate the vergence-accommodation conflict, developed machine learning-based gaze prediction models and worked on eye-tracked user interfaces. He has previously co-organised two SIGGRAPH courses (Attention-Aware Rendering, Mobile Graphics and Games in 2014, Applications of Visual Perception to Virtual Reality Rendering in 2017).



Katerina Mania serves as an Associate Professor at the School of Electrical and Computer Engineering, Technical University of Crete, Greece after research positions at HP Labs, UK where she worked on Web3D and University of Sussex, UK where she served as an Assistant Professor in Multimedia Systems. She received her BSc in Mathematics from the University of Crete, Greece and her MSc and PhD in Computer Science from the University of Bristol, UK. Her primary research interests integrate perception, vision and neuroscience to optimise computer graphics rendering and VR technologies with current focus on gaze-contingent displays. She has co-chaired technical programs and has participated in over 100 international conference program committees. She serves as one of the Associate Editors for Presence, Tele-operators and Virtual Environments (MIT Press) and ACM Transactions on Applied Perception.



Rafał K. Mantiuk is a Reader (Associate Professor) at the Department of Computer Science and Technology, University of Cambridge (UK). He received his PhD from the Max-Planck-Institute for Computer Science (Germany). His recent interests focus on computational displays, novel display technologies, rendering and imaging algorithms that adapt to human visual performance and viewing conditions in order to deliver the best images given limited resources, such as computation time, bandwidth or dynamic range. He contributed to early work on high dynamic range imaging, including quality metrics (HDR-VDP), video compression and tone-mapping.



Christian Richardt is a Lecturer (Assistant Professor) and EPSRC-UKRI Innovation Fellow at the University of Bath, UK. He received a BA and PhD in Computer Science from the University of Cambridge. He was previously a postdoctoral researcher at Inria Sophia Antipolis, Max Planck Institute for Informatics and the Intel Visual Computing Institute. His research combines insights from vision, graphics and perception to extract and reconstruct visual information from images and videos, to create high-quality visual experiences with a focus on 6-degree-of-freedom VR video. He has previously co-organised two SIGGRAPH courses (User-Centric Videography in 2015, Video for Virtual Reality in 2017).



Michael Stengel is working as a Research Scientist with Nvidia since 2017. His research is focused on perceptual aspects in Computer Graphics, in particular hardware and algorithms for gaze-contingent displays and real-time rendering. Michael Stengel received a Diploma in Computational Visualistics from University of Magdeburg, Germany (2011) and holds a Ph.D. degree in Computer Science from TU Braunschweig, Germany (2016). In 2010 he joined the Virtual Reality Lab at Volkswagen AG, Wolfsburg, Germany where he developed haptics algorithms for immersive rendering. As a postdoctoral research scientist he worked in 2016 and 2017 with TU Delft and VU Medical Center, Amsterdam in the Netherlands where he worked on subject monitoring during awake brain surgeries.